CHIMIKA CHRONIKA

NEW SERIES

AN INTERNATIONAL EDITION
OF THE ASSOCIATION OF GREEK CHEMISTS

CMCRCZ 19(2), 65-124(1990)

ISSN 0366-693X

2/90

Volume 19, No 2, p.p. 65-124 June 1990

CHIMIKA CHRONIKA
NEW SERIES
AN INTERNATIONAL EDITION

Pübished by the Association of Greek Chemists (A.G.C.)
27 Kaningos str. Athens 106 82 Greece

Journals Managing Committee, A.G.C.:
P.A. Siskos (Coordinator)
A. Cosmatos, P.N. Dimotakis, D. Hatzigeorgiou-Giannakaki, M. Kazanis, Ch. Noumptas, M. Petropoulou-Ochsenkühn, E. Sakki, R. Scoulica, Th. Vakirtzi, E. Voudouris.

Editor-in-chief: P.N. Dimotakis
Editors: N. Alexandrou, A. Cosmatos, A. Evangelopoulos, N. Hadjiliadis, N. Hadjichristidis, M.I. Karayannis, N. Katsanos, J. Petropoulos, D. Tassios.

Foreign Advisors: P. Bontchev (Sofia), H. Işçi (Ankara), G.M. Milanovic (Belgrade), E. Plasari (Tirana), K.C. Nikolaou (Cyprus).

Correspondence, submission of papers, subscriptions, renewals and changes of address should be sent to Chimika Chronika - New Series, 27 Kaningos street, Athens 106 82, Greece. The Guide to Authors is published in the first issue of each volume, or sent by request. Subscriptions are taken by volume at 1000 drachmas for membres and 2000 drachmas for Corporations in Greece and 28 U.S. dollars to all other countries except Cyprus, where subscriptions are made on request.

Phototypesetted and Printed in Greece by LICHNOS LTD GRAPHIC ARTS
24, PL. THEATROU 105 52 ATHENS tel. 3214766

Υπεύθυνος σύμφωνα με το νόμο: Νίκος Κατσαρός, Κάνιγγος 27, Αθήνα 106 82.

Chimika Chronika, New Series,. 19, 65-79(1990)

MOLECULAR ORBITAL INVESTIGATION OF THE CATALYTIC ACTIVITY OF SOME IRON(III) HALOBISDITHIOCARBAMATES AND THEIR MÖSSBAUER SPECTRA

E.G. BAKALBASSIS, G.A. KATSOULOS, M.P. SIGALAS and C.A. TSIPIS

Department of General and Inorganic Chemistry, Aristotle University, Thessaloniki 54006, Greece.

(Received January 14, 1988)

SUMMARY

EHMO-SCCC calculations have been used in the analysis of the electronic structure and related properties of some iron(III) halobisdithiocarbamates. Based on the molecular orbital description of complexes and the frontier molecular orbital approach of chemical reactivity, a qualitative interpretation of their ability to act as potential catalysts for halogen addition reactions to alkenes has been deduced. The extended-Hückel molecular orbital approach has been also used for the consideration of the structure of the tetrameric halogeno bridging unit of the corresponding binuclear Fe(III) dithiocarbamates which can be regarded as the active species in the aforesaid homogeneous catalytic reactions. The rough features of the shape of the bridging unit are discussed in terms of the molecular orbital pictures and energy-level correlation diagrams deduced from the rule of maximization of overlap and orbital symmetry considerations. Finally, the electric field gradient at the metal nucleus in the precursor mononuclear complexes has been computed with the aid of quantum-chemical calculations and found to be in good agreement with the experimental values.

Key words: Binuclear complexes. Bridging unit. Dithiocarbamates. Mössbauer spectra. Quantum-chemical calculations. Walsh diagrams.

INTRODUCTION

Recently, we reported[1-4] on the treatment of iron(III) halobisdithiocarbamates with molecular halogens resulting in the formation of homobinuclear complexes formulated as $[Fe(R_2dtc)_2X]_2(\mu\text{-}X'_2)$, where R = Me, Et, Pr^i; X = Cl, Br, I, and X′ = Br, I. A loose dimeric association of the type $(R_2dtc)_2FeX\cdots X'\text{-}X'\cdots XFe(R_2dtc)_2$ has been confirmed by spectroscopic,[1,5,6] magnetic[7] and thermoanalytical[2,4] studies on these novel com-

pounds. In particular, the molecular halogen interacts weakly in an end-to-end fashion with the halide ligand of the mononuclear complexes affording an extended tetrameric bridging unit, $\{X\text{-}X'\text{-}X'\text{-}X\}^{2-}$, between the two paramagnetic centers. These conclusions are consistent with the X-ray crystal structure determination of a complex of this series containing the pyrrolidinyldithiocarbamato ligand.[8] Moreover, these binuclear dihalide-bridged iron(III) complexes can be regarded as potential carriers of activated molecular halogens and hence could be the active species in homogeneous catalytic halogen addition reactions to alkenes in the presence of iron(III) halobisdithiocarbamates.[9] Actually, we have found that under mild conditions (20°C) and relatively low catalyst concentrations (10^{-2}-10^{-3} mol catalyst·mol alkene^{-1}) the iron(III) halobisdithiocarbamates promote the ready addition of molecular halogens to alkenes in CH_2Cl_2 solutions affording the corresponding *cis*-addition products.[9] This catalytic effect may be due to dimer formation.

In order to investigate further the activation of the molecular halogen in the bridging dimers we have carried out a systematic structural study of the tetrameric bridging unit $\{I\text{-}I\text{-}I\text{-}I\}^{2-}$ within the framework of the extended-Hückel molecular orbital approach (EHMO). The simplicity, utility and economy of the EHMO calculations over a wide range of geometries has been well-proven in studies of the borane and related systems, as well as conventionally coordinated species.[10] Furthermore, the EHMO approach, in conjunction with the Jahn-Teller theorem, has been shown to be a powerful tool for both the prediction and rationalization of cluster structures and the understanding of stereochemical non-rigidity in solution.[11,12] It is Walsh's general approach,[13] aided by energy levels and orbitals,[14-16] that is used here for the determination of the rough features of the shapes of the extended tetrameric halogeno bridging unit. Consequently, orbital pictures and energy level diagrams along with simple physical rationalizations, which make the shapes of this bridging unit understandable from a molecular orbital point of view, are presented in this paper. Moreover, an insight concerning the structural and bonding properties of the precursor mononuclear complexes forming the magnetic dimers, was gained through EHMO calculations. In this respect, an attempt was also made to calculate the electric field gradient (EFG) and quadrupole splitting (QS) values for the above five-coordinated iron(III) dithiocarbamato complexes.

COMPUTATIONAL DETAILS

The single electron molecular functions of the $[Fe(Et_2dtc)_2X]$ complexes (X = Cl, Br, I) were calculated by means of the LCAO-MO method[17-19] with self-consistent charge and configuration (EHMO-SCCC) by using option 3 of the FORTICON-8 computer program.[20] In these iterative calculations the "weighted H_{ij} formula" for the off-di-

agonal matrix elements (H_{ij}) was used;[21] still a Madelung energy correction[20,22,23] was applied to the diagonal matrix elements, H_{ii}. The value of 1.75 was used for the parameter K, as this value was found by a series of calculations to give the best agreement between the experimental and theoretical frequencies of the ligand-field bands of the complexes studied.[24,25] With the exception of the iron 3d orbitals, which were represented by double-exponent functions, single-exponent Slater type orbitals for sulphur, carbon, nitrogen, and hydrogen were used.[20] The sulphur d AO's were not included in the basis set of the complexes as their contribution was found to be insignificant. Moreover, the single-Slater type orbital exponents for Cl, Br, and I used were 2.033 (3s and 3p), 2.64 (4s and 4p), and 2.68 (5s and 5p), respectively.[20,26]

The geometries of the $[Fe(Et_2dtc)_2Cl]$, **1**, $[Fe(Et_2dtc)_2Br]$, **2**, and $[Fe(Et_2dtc)_2I]$, **3**, complexes were taken from their crystal-structure determinations.[27-29] Furthermore, to limit the calculation time and the basis set, the ethyl groups of the dithiocarbamato ligands were substituted by hydrogen atoms, the bond length value of N-H being 1.01 Å.[30] The three complexes were regularized to give approximately C_{2v} symmetries and the coordinate system adopted was in accordance with the symmetry rules.

The $\{I\text{-}I\text{-}I\text{-}I\}^{2-}$ calculations that underlie the arguments used in this paper were also of the extended Hückel type. Both 5s and 5p exponents for I were taken as 1.90; still the H_{ii} values (eV) were H_{ss} = -22.00 and H_{pp}=-10.27. The geometry of the molecule enters the calculation through the overlap integrals, which depend on the internal interatomic coordinates. From the dependence of H_{ij} on overlap, it follows that if a change in the molecular geometry increases the overlapping between the atomic orbitals involved in a particular molecular orbital, this fact will stabilize that MO. In the calculations required for this paper, bond lengths were kept fixed at experimental values or reasonable estimates; still the bond angles were varied to find the geometry minimizing the total energy, E.

RESULTS AND DISCUSSION

Bonding of the Complexes.

The calculated eigenvalues, charge distribution and partial wave analyses of the molecular orbitals of main interest for the complexes under investigation, in their paramagnetic quartet ground states are listed in Tables I-III. The occupied valence MO's have energies in the range -31.55 to -9.13 eV's. There is an efficient mixing of metal and ligand orbitals for all complexes. Moreover, it should be stressed that there is an efficient mixing of the $4p_z$ and $3d_{z^2}$ AO's of the central atom in the $11a_1$ SOMO's, due to the contribution of the $4p_z$ AO in the formation of the Fe-X axial bonds of the complexes. Except

for an inversion between the $3d_{z^2}$ and $3d_{yz}$ AO's in **3**, there is a large similarity between the energy-level schemes of the complexes, the sequence of the predominantly 3d orbitals localized mainly on the central atom being $3d_{xy} > 3d_{z^2} > 3d_{yz} > 3d_{xz} > 3d_{x^2-y^2}$.

TABLE I. Eigenvalues and Character of the Valence MO's of Main Interest of the [Fe-$(R_2dtc)_2Cl$] Complex.[a]

Level[b]	Energy (eV)	Charge Distribution[c] (%)				Basis Functions		
		Fe	Cl	4S	L	Fe	Cl	S
$14b_1$	63.19	88	0	8	4	x,xz		s,y,z
$17a_1$	45.57	58	0	24	18	s,z		s,x,y
$10b_2$	42.11	91	0	9	0	y,yz		s,x
$15a_1$	27.40	88	6	3	3	z,s	s,z	z
$8a_2$	13.90	2	0	46	52	xy		y,s,x
$6a_2$	-5.98	40	0	58	2	xy		y,x
$10b_1$	-7.18	5	0	36	59	xz		z,x
$12a_1$	-7.88	10	2	24	64	z^2	s,z	z
$11a_1$	-9.93	67	17	2	14	z^2,z	z	
$7b_2$	-10.04	67	4	26	3	yz,y	y	x,y
$9b_1$	-10.39	72	8	8	12	xz	x	x
$10a_1$	-10.64	97	0	0	3	x^2-y^2		
$6b_2$	-11.20	17	0	77	6	yz		y,z
$5a_2$	-11.48	8	0	92	0	xy		x,z
$5b_2$	-11.56	0	93	5	2		y	y
$8b_1$	-11.60	8	90	0	2	xz	x	
$9a_1$	-11.88	19	81	0	0	z^2	z	
$4a_2$	-11.93	30	0	60	10	xy		y,z
$4b_2$	-12.87	16	2	80	2	yz		z
$3b_1$	-19.08	3	0	36	61	x		s
$4a_1$	-19.68	5	0	42	53	s		s
$3a_1$	-23.99	7	91	0	2	z	s	
$1b_2$	-24.17	3	0	83	14	y		s
$1b_1$	-31.46	0	0	13	87			s

[a] The valence molecular orbital listed are only those associated with both the central atom and ligand valence AO's. [b] The highest occupied level is $11a_1$. [c] Percentage of the MO's total population located on the indicated atoms or group of atoms.

The in-plane σ-bonding of the complexes results mainly from the bonding $4a_2$, $5a_2$ and the antibonding $6a_2$ and $8a_2$ MO's having substantial metal and sulphur-ligand character. Due to the greater stabilization of both A_2 and B_2 MO's for **3** as compared to the ones of **2** and **1** the following trend of the Fe-S bond strength could be proposed: $Fe\text{-}S_{(I)}$

> $Fe\text{-}S_{(Br)}$ > $Fe\text{-}S_{(Cl)}$. This is further supported by the two-center energy terms and the overlap population values of the compounds under investigation (Table IV). This trend is

TABLE II. Eigenvalues and Character of the Valence MO's of Main Interest of the [Fe-$(R_2dtc)_2Br$] Complex.[a]

Level[b]	Energy (eV)	Charge Distribution[c] (%)				Basis Functions		
		Fe	Br	4S	L	Fe	Br	S
$14b_1$	65.68	89	0	7	4	x,xz		s,y,z
$17a_1$	44.40	64	0	20	16	s,z		s,y,x
$10b_2$	42.62	91	0	9	0	y,yz		s,x,z
$15a_1$	20.80	83	5	6	6	z,s	s	z
$8a_2$	12.83	2	0	45	53	xy		y,s,x
$6a_2$	-5.59	41	0	57	2	xy		x,y
$10b_1$	-6.96	5	0	33	62	xz		z,x
$12a_1$	-7.66	10	3	22	68	z^2	z	z
$11a_1$	-9.47	61	23	2	14	z^2,z	z	
$7b_2$	-9.60	66	5	26	3	yz	y	y
$9b_1$	-9.94	72	11	7	10	xz	x	x
$10a_1$	-10.22	97	0	0	3	$x^2\text{-}y^2$		
$6b_2$	-10.79	19	6	70	5	yz	y	y,z
$5b_2$	-10.96	0	86	12	2		y	y
$8b_1$	-11.01	10	86	0	4	xz	x	
$5a_2$	-11.16	14	0	86	0	xy		x,z,y
$9a_1$	-11.41	28	72	0	0	z^2	z	
$4a_2$	-11.53	24	0	66	10	xy		y,z
$4b_2$	-12.48	15	2	82	1	yz		z
$3b_1$	-19.00	3	0	32	65	x		s
$4a_1$	-19.56	5	0	38	57	s		s
$3a_1$	-22.72	6	93	0	1	z	s	
$1b_2$	-23.76	4	0	84	2	y		s
$1b_1$	-31.55	0	0	11	89			s

[a,b,c] See footnotes, Table I.

in accordance with the greater electronegativity of the Cl atom as compared to those of Br and I ones, which in turn can afford to a decrease in the electron population on the Fe-S bonds of complex **1**.

Finally, the out-of-plane π-bonding results mainly from the bonding $4b_2$ and the antibonding $7b_2$ MO's for **1** and **2**, and the $5b_2$ and $9b_2$ MO's for **3**.

TABLE III. Eigenvalues and Character of the Valence MO's of Main Interest of the [Fe-$(R_2dtc)_2I$] Complex.[a]

Level[b]	Energy (eV)	Charge Distribution[c] (%)				Basis Functions		
		Fe	I	4S	L	Fe	I	S
$12b_1$	72.12	86	0	10	4	x,xz		s,y,z
$17a_1$	46.77	61	0	22	17	s,z		s,y,x
$12b_2$	42.85	89	0	11	0	y		s,x,z
$15a_1$	24.64	83	8	5	4	z,s	s,z	z,y
$8a_2$	14.16	2	0	48	50	xy		x,s,y
$6a_2$	-5.10	41	0	56	3	xy		x,y
$8b_1$	-7.01	7	0	32	61	xz		z,x
$12a_1$	-7.41	14	8	22	56	z^2	z,s	z
$9b_2$	-9.20	62	8	27	3	yz	y	y,x
$11a_1$	-9.25	51	25	2	22	z^2,z	z	
$7b_1$	-9.54	64	21	7	8	xz	x	x
$10a_1$	-9.84	98	0	0	2	x^2-y^2		
$8b_2$	-10.28	10	80	10	0	yz	y	z
$6b_1$	-10.40	17	78	0	5	xz	x	
$7b_2$	-10.44	15	10	68	7	yz	y	y,z
$9a_1$	-10.84	36	64	0	0	z^2	z	
$5a_2$	-10.88	28	0	70	2	xy		z,y,x
$4a_2$	-11.29	11	0	81	8	xy		y,z
$5b_2$	-12.23	14	2	84	0	yz		z
$3b_1$	-18.65	4	0	36	60	x		s,y
$4a_1$	-19.25	6	0	40	54	s		s,x,y
$3a_1$	-22.36	8	91	0	1	z	s,z	
$1b_2$	-23.64	6	0	82	12	y		s,y
$1b_1$	-30.95	0	0	12	88			s

[a,c] See footnotes, Table I. [b] The highest occupied level is $9b_2$.

Calculation of the QS and η Values.

Mössbauer spectral data for some of the halobis(N,N-dialkyldithiocarbamato)iron-(III) complexes have been obtained previously.[24,25,31-33] There was no systematic variation in the isomer shifts (IS) which were all close to 0.64 mm·sec^{-1} (with respect to sodium nitroprusside) at room temperature, but the quadrupole splitting (QS), although independent of R, showed a strong dependence on the nature of X and ranged from 2.4 to 3.0 mm·sec^{-1}. The constancy of the isomer shift with varying X was explained with respect to the inability of the halide ligands to act simultaneously as π-donors in these

compounds.[25] Although the origin of the splitting has been worked out theoretically and it was shown that the abnormally large electric field gradient (EFG) in $[Fe(Et_2dtc)_2Cl]$ was mainly caused by covalency effects,[34] no explanation has been given for the remarkable dependence of the QS on the nature of the halide ligand. However, the spectral data

TABLE IV. Two-Center Energy Terms and Overlap Population for the Coordination Bonds of the Compounds under Investigation.

Compound	Fe-X	Energy (eV)	Overlap Population
$[Fe(R_2dtc)_2Cl]$	Fe-S	-3.3743	0.2832
	Fe-Cl	-4.1009	0.3297
$[Fe(R_2dtc)_2Br]$	Fe-S	-3.5281	0.3023
	Fe-Br	-3.5847	0.3323
$[Fe(R_2dtc)_2I]$	Fe-S	-4.2852	0.3646
	Fe-I	-4.6320	0.4429

are consistent with an orientation of the major axis of the EFG parallel to the Fe-X direction,[35] and hence the regular decrease of splitting from I^- to Cl^- may be interpreted with respect to the contribution due to X^-. To this end we have computed the $[Fe(R_2dtc)_2X]$ (X = Cl, Br, I) molecular orbitals (MO) taking into account all the valence electrons. Actually, the theoretical values of the quadrupole splitting (QS) and asymmetry parameter (η) have been calculated from atomic orbital net populations, as outlined by de Vries.[34] According to this method, the asymmetry parameter, $\eta = (V_{zz}-V_{yy})/V_{zz}$, can be deduced from the resulting V_{zz} and $V_{zz}-V_{yy}$, obtained by summing the 3d and 4p contributions, whereas the QS is calculated from $QS = \frac{1}{2}e\cdot V_{zz}\cdot Q(1+\eta^2/3)^{1/2}$, Q being the nuclear quadrupole moment of the ^{57}Fe first excited nuclear state,[36] equal to 0.21±0.03 barn. For the core-orthogonalized Slater type orbitals $\langle r^{-3}\rangle_{3d} = 32.0$ Å^{-3} and $\langle r^{-3}\rangle_{4p} = 11.6$ Å^{-3}, while the value of 0.32 was used for the Sternheimer factor R_{3d}.[37]

However, some unreliability of the results may be caused by the inaccuracy of the input parameters, especially the $\langle r^{-3}\rangle_{3d}$ value. Therefore, following Karplus and Pople,[38] we assumed that this mean distance can be calculated by extending the Slater rules to fractional electron populations.[39] For a valence electron density P_{3d} on Fe atom this gives $Z^*_{3d} = 13.2-0.35(P_{3d}-1)$, Z^*_{3d} being the effective nuclear charge. For a Slater 3d orbital, $\langle r^{-3}\rangle_{3d}$ is now given by $\langle r^{-3}\rangle_{3d} = (1/405)Z^{*3}_{3d}$.

TABLE V. Net Orbital Populations of the Complexes Studied and Resulting EFG and QS.

AO	Net Orbital Populations		
	$[Fe(R_2dtc)_2Cl]$	$[Fe(R_2dtc)_2Br]$	$[Fe(R_2dtc)_2I]$
$4p_x$	0.1290	0.1322	0.1431
$4p_y$	0.0294	0.0308	0.0484
$4p_z$	0.0430	0.0387	0.0546
$3d_{x^2-y^2}$	2.0068	2.0054	2.0137
$3d_{z^2}$	1.1163	1.1737	1.1745
$3d_{xy}$	0.9777	0.9612	0.9540
$3d_{xz}$	1.1545	1.1494	1.1839
$3d_{yz}$	1.3005	1.3052	1.3469
$3d_{x^2-y^2}$-$3d_{z^2}$	0.0166	0.0261	0.0492
V_{zz}[a]	1.154[d]	1.019	0.9505
	(1.187)[e]	(1.058)	(0.988)
η[b]	0.43	0.57	0.79
	(0.30)	(0.42)	(0.625)
QS[c]	2.60	2.35	2.29
	(2.64)	(2.38)	(2.30)

[a] Z component of EFG in 10^{22} V·m^{-2}. [b] Asymmetry parameter, $\eta = (V_{zz}-V_{yy})/V_{zz}$. [c] Quadrupole splitting in mm·sec^{-1}, calculated with Q = 0.21 ± 0.03 barn. [d] Values calculated taking into account only the contribution of 3d atomic orbital populations to the EFG. [e] Values in parentheses were calculated taking into account the contribution of all iron valence orbitals to the EFG.

It is important to note that the use of this expression for the calculation of $\langle r^{-3}\rangle_{3d}$ immediately introduces a small dependence of the calculated QS on the total electron density on Fe atom in each complex. As a matter of fact it was shown that this $\langle r^{-3}\rangle_{3d}$ electron density correlation increases the reliability of the calculated electric field gradient values. Table V gives the net populations of the 3d and 4p atomic orbitals of Fe(III) along with the computed and the experimental QS and η values of the complexes under investigation. Due to the substantial participation of the 4p AO's in the bonding of the complexes, the EFG values were calculated either by taking into account or not the 4p atomic orbital populations. From the examination of these results, a reasonable agreement between the calculated and experimental QS and η values is derived, despite the simplistic approach adopted in our calculations.

The Structure of the Tetrameric Halogeno Bridging Unit.

On the basis of the qualitative MO model of molecular shapes and electronic structure, formulated by Mulliken and Walsh,[13,40] it is the energetic behaviour of the HOMO on distortion that determines the molecular geometry. Therefore, we attempted to deduce the point group to which the I_4^{2-} framework belongs by a balance of maximizations of overlaps among the AO's in the occupied MO's. To this end the following geometries

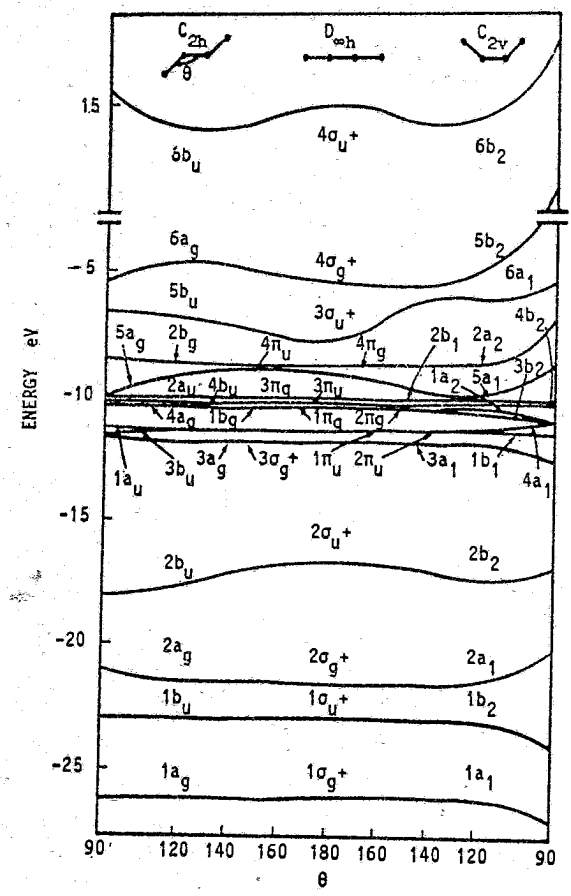

FIG. 1. *Correlation diagram for I_4^{-2} orbital energies in linear, cis, and trans geometries.*

were investigated for the tetrameric halogeno bridging unit; the linear ($D_{\infty h}$), and the planar with *cis* (C_{2v}) and *trans* (C_{2h}) conformers. Fig. 1 is a correlation diagram representing the way the MO energy levels change with symmetric *cis* or *trans* bending, compared

to those for linear geometry. For the 30-electron system it is not immediately clear from this orbital diagram what geometry is preferred. Numerically, however, by weighting the calculated energy levels with the number of electrons in each orbital, the linear geometry wins out. With hindsight we could argue that on going to the *trans* planar structure the energy gain associated with $2b_u$ and $5a_g$ is canceled out by the rise in energy of $5b_u$ and $6a_g$ and so the energetics are controlled by $2a_g$. In the *cis* planar configuration all $2a_1$, $6a_1$ and $5b_2$ rise in energy on distortion, making thus impossible the nonlinear geometry. These principal atomic orbitals which make up each of the valence molecular orbitals of the model I_4^{2-} species in linear and bent configurations are shown schematically in Fig. 2.

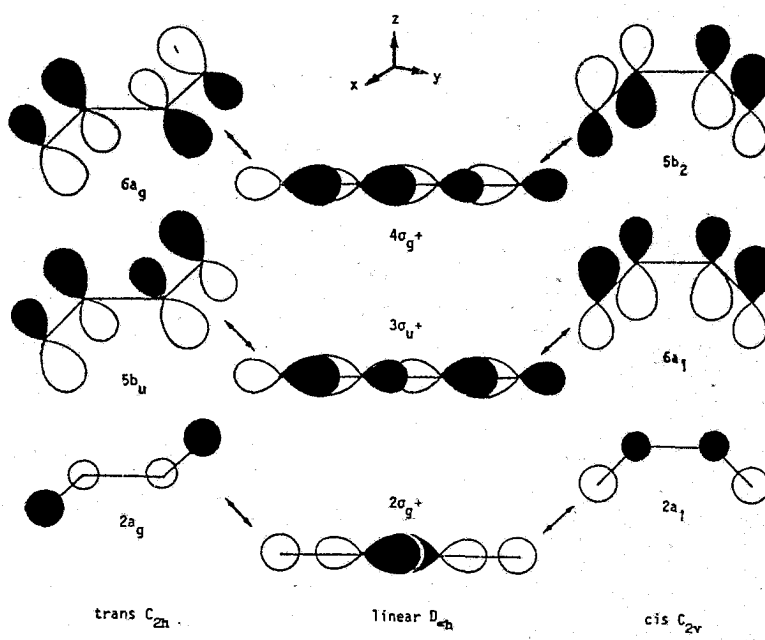

FIG. 2. *The $2\sigma_g^+$, $3\sigma_u^+$, $4\sigma_g^+$, and related valence orbitals for the I_4^{-2} anion.*

Finally, in Fig. 3 the total energy E as a function of angles for the 30-electron system in the I_4^{2-} framework in *cis, trans* and linear shapes, is presented.

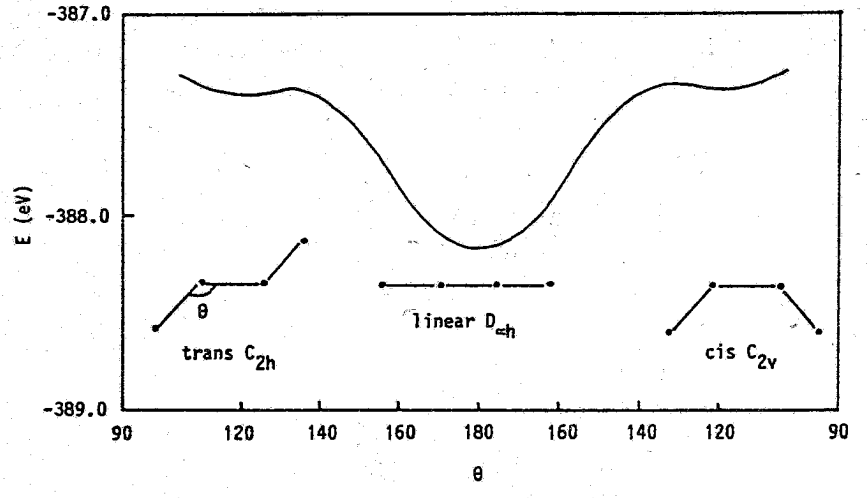

FIG. 3. *Total energy of the 30-electron system in the I_4^{-2} framework in cis, trans, and linear shapes.*

Ground-State Properties and Mechanisms.

In view of the fact that the nucleophilic substitution reactions occur through FMO interactions, a qualitative interpretation of some important ground-state properties of the compounds under investigation could be easily emerge based upon the quantum-chemical results.

It was verified experimentally that complex **3** reacts with the I_2 molecule to give the dihalide-bridged iron(III) dithiocarbamate.[1,2,5-7] This is not surprising if we take into account the character and energy differences of their frontier MO's. It is evident from Table III, that all SOMO's of the $[Fe(Et_2dtc)_2I]$ complex are mainly localized on Fe d AO's (d_{z^2}, d_{yz}, and d_{xz}) and halogen p AO's (p_z, p_y, and p_x), as well. Moreover, the LUMO of this complex did not exhibit any appreciable character of metal or halogen AO functions. Therefore, the only short-range allowed interactions between the iodide ligand of $[Fe(Et_2dtc)_2I]$ and the I_2 molecule should be those between the SOMO's of **3** and the HOMO or LUMO of the latter. However, the LUMO of the iodine is localized on the s and p_x AO's of its atoms; its HOMO being localized on their p_y and p_z AO's. Hence, the homobinuclear iron(III) complex could be easily derived either through a SOMO-HOMO and/or a SOMO-LUMO interaction. Accordingly, a question arises concerning the possible mechanism of the reaction of $[Fe(R_2dtc)_2I]$ with the molecular iodine. Fig. 4 shows all possible orbital interactions. Actually, the $SOMO_3$-LUMO interaction could lead to a

σ-type $\{Fe(R_2dtc)_2I\text{-}I_2\}$ bond, whereas the $SOMO_1$-HOMO and $SOMO_2$-HOMO interactions could lead to π-type $\{Fe(R_2dtc)_2I\text{-}I_2\}$ bonds. Consequently, through a new $SOMO_3$-LUMO, $SOMO_1$-HOMO and/or $SOMO_2$-HOMO interactions, the dihalide-bridged $(R_2dtc)_2FeI\cdots I\text{-}I\cdots IFe(R_2dtc)_2$ dimer could be possibly derived.

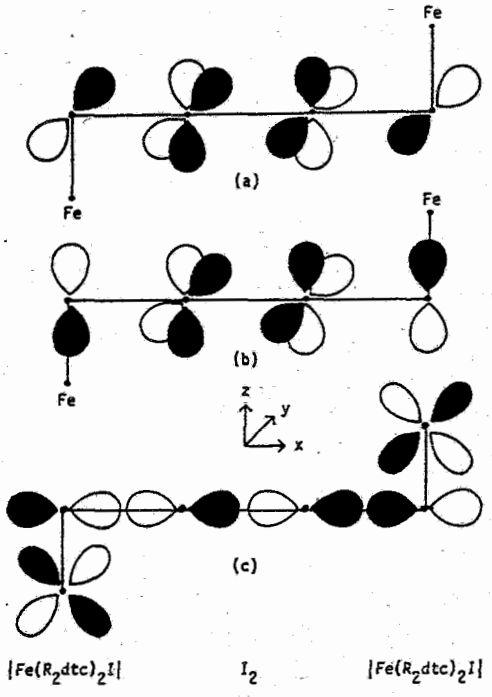

FIG.4. *First order exchange interactions between the [Fe(Et$_2$dtc)$_2$I] complex and the iodine molecule: (a) SOMO$_1$-HOMO, (b) SOMO$_2$-HOMO, and (c) SOMO$_3$- LUMO.*

Within the framework of the same quantum-chemical results the catalytic addition of molecular halogens to alkenes in the presence of $[Fe(R_2dtc)_2I]$ could be also considered.

It was verified experimentally that the binuclear iron(III) complexes react readily with alkenes, such as ethylene and cyclohexene, to afford *cis*-addition products according to the scheme:[1,3,9]

$$[Fe(S_2CNR_2)_2I]_2{\cdot}I_2 + >C{=}C< \rightarrow 2\,[Fe(S_2CNR_2)_2I] + >IC\text{-}CI<$$

The easy addition of the iodine indicates that this molecule must be activated by its association to the $[Fe(S_2CNR_2)_2I]$ complex, a process which is a necessary step in the addition reactions. Actually, the Mulliken population analysis on the linear tetratomic

bridging unit $\{I\text{-}I\text{-}I\text{-}I\}^{2-}$ showed that the bond order of the central I-I bond is only 0.530, a fact which is in accordance with the activation of the molecular iodine in the binuclear complex. Therefore, we thought that the iron(III) halobisdithiocarbamates could be active

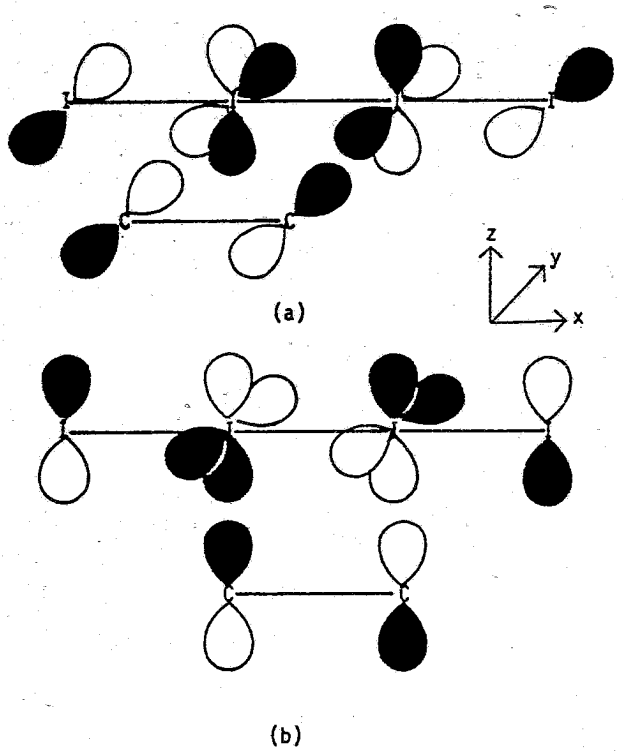

FIG. 5. *FMO interactions between the tetrameric halogeno bridging unit and the ethylene molecule: (a) on xy plane, and (b) on yz plane.*

as homogeneous catalysts for halogen addition reactions to olefins. A catalytic cycle involving a four-center transition state has already been proposed by us.[9] The frontier MO's interactions between the tetrameric halogeno bridging unit and the ethylene molecule, responsible for the formation of the transition state are depicted schematically in Fig. 5. However, in this transition state, due to steric hindrances, a direct frontier-controlled attack of the ethylene molecule to the central I-I bond of the linear tetratomic bridging unit could effectively happen only on the xy plane. This orientation provides the best NNHOMO-LUMO overlapping, leading to the formation of the carbon-iodide σ-bonds. This could lead to an electronic rearrangement in the system followed by a weak-

ening of the two terminal FeI-I bonds and the concomitant cleavage of the 1,2-addition product.

ΚΒΑΝΤΟΧΗΜΙΚΗ ΜΕΛΕΤΗ ΤΗΣ ΚΑΤΑΛΥΤΙΚΗΣ ΔΡΑΣΤΙΚΟΤΗΤΑΣ ΚΑΙ ΤΩΝ ΦΑΣΜΑΤΩΝ MÖSSBAUER ΑΛΟΓΟΝΟΔΙΘΕΙΟΚΑΡΒΑΜΙΔΙΚΩΝ ΣΥΜΠΛΟΚΩΝ ΤΟΥ ΣΙΔΗΡΟΥ(III) - Στην εργασία αυτή μελετήθηκαν, με βάση την κβαντοχημική μέθοδο extended Hückel LCAO-MO, η ηλεκτρονική δομή και οι δεσμικές ιδιότητες τριων αλογονοδιθειοκαρβαμιδικών συμπλόκων του σιδήρου(III), του γενικού τύπου $[Fe(R_2dtc)_2X]$, όπου X = Cl, Br ή I. Η μελέτη αυτή έγινε προκειμένου να εξακριβωθεί ο μηχανισμός αλληλεπίδρασης των συμπλόκων αυτών με μοριακό αλογόνο (X′ = Br ή I), ο οποίος οδηγεί στο σχηματισμό μαγνητικών διπυρηνικών συστημάτων του γενικού τύπου $[Fe(R_2dtc)_2X]_2(\mu\text{-}X'_2)$. Τα συστήματα αυτά χαρακτηρίζονται από την παρουσία ενός εκτεταμένου δεσμού τεσσάρων κέντρων, X···X′-X′···X, του οποίου επιχειρήθηκε να διαπιστωθεί η στερεοχημική διαμόρφωση με βάση τη μέθοδο Walsh, η οποία στηρίζεται στη δημιουργία ενεργειακών διαγραμμάτων σε συνάρτηση με τη μεταβολή κάποιας δομικής παραμέτρου. Επιπλέον, οι κβαντοχημικοί υπολογισμοί επέτρεψαν να προταθεί ένας πιθανός μηχανισμός για την προσθήκη μοριακών αλογόνων σε αλκένια, με την παρουσία μιας καταλυτικά δρώσας ποσότητας του συμπλόκου $[Fe(R_2dtc)_2X]$. Τέλος, έγινε προσπάθεια για το θεωρητικό υπολογισμό των παραμέτρων Mössbauer των μονοπυρηνικών αλογονοδιθειοκαρβαμιδικών συμπλόκων, η οποία οδήγησε σε μια πολύ ικανοποιητική συμφωνία με τις αντίστοιχες πειραματικές τιμές.

REFERENCES

1. Katsoulos, G.A., Tsipis, C.A. and Vakoulis, F.D.: *Can. J. Chem.*, **63**, 3249 (1985).
2. Lalia-Kantouri, M., Katsoulos, G.A. and Vakoulis, F.D.: *J. Thermal Anal.*, **31**, 447 (1986).
3. Vakoulis, F.D., Katsoulos, G.A. and Tsipis, C.A.: *Inorg. Chim. Acta*, **112**, 139 (1985).
4. Katsoulos, G.A., Lalia-Kantouri, M. and Vakoulis, F.D.: *J. Thermal Anal.*, **31**, 537 (1986).
5. Pasek, E.A. and Straub, D.K.: *Inorg. Chim. Acta*, **21**, 23 (1977).
6. Petridis, D., Kostikas, A., Simopoulos, A. and Niarchos, D.: *Inorg. Chem.*, **21**, 766 (1982).
7. Vakoulis, F.D.: *Ph.D. Thesis*, University of Thessaloniki (1984).
8. Kepert, D.L., Raston, C.L., White, A.H. and Petridis, D.: *J. Chem. Soc., Dalton Trans.*, 1921 (1980).
9. Tsipis, C.A., Katsoulos, G.A. and Vakoulis, F.D.: *J. Chem. Soc., Chem. Comm.*, 1404 (1985).
10. Muetterties, E.L., Hoel, E.L., Salenture, C.G. and Hawthorne, M.F.: *Inorg. Chem.*, **14**, 950 (1975).
11. Muetterties, E.L. and Beier, B.F.: *Bull. Soc. Chim. Belg.*, **84**, 397 (1975).
12. Burns, R.C., Gillespie, R.J., Barnes, J.A. and McGlinchey, M.J.: *Inorg. Chem.*, **21**, 799 (1982).
13. Walsh, A.D.: *J. Chem. Soc.*, 2260 (1953).
14. Gimarc, B.M.: *J. Am. Chem. Soc.*, **92**, 266 (1970).
15. Gimarc, B.M.: *J. Am. Chem. Soc.*, **93**, 593 (1971).
16. Gimarc, B.M.: *J. Am. Chem. Soc.*, **93**, 815 (1971).

17. Hoffmann, R.: *J. Chem. Phys.*, **39**, 1937 (1963).
18. Viste, A. and Gray, H.B.: *Inorg. Chem.*, **3**, 1113 (1964).
19. Ballhausen, C.J. and Gray, H.B.: *Inorg. Chem.*, **1**, 111 (1962).
20. Howell, J., Rossi, A., Wallace, D., Haraki, K. and Hoffmann, R.: "FORTICON-8", Q.C.P.E. No. 344, Indiana University.
21. Ammeter, J.H., Burgi, H.B., Thibeault, J.C. and Hoffmann, R.: *J. Am. Chem. Soc.*, **100**, 3686 (1978).
22. Ohno, K.: Theor. Chim. Acta, 86, 1463 (1964).
23. Klopman, G.: *J. Am. Chem. Soc.*, **86**, 1464, 4550 (1964).
24. De Vries, J.L.K.F., Trooster, J.M. and De Boer, E.: *Inorg. Chem.*, **10**, 81 (1971).
25. Epstein, L.M. and Straub, D.K.: *Inorg. Chem.*, **8**, 560 (1969).
26. Van der Velden, J.W.A. and Stadnik, Z.M.: *Inorg. Chem.*, **23**, 2640 (1984).
27. Hoskins, B.F. and White, A.H.: *J. Chem. Soc. (A)*, 1668 (1970).
28. Chapps, G.E., McCann, S.W. and Wickman, H.H.: *J. Chem. Phys.*, **60**, 990 (1974).
29. Healy, P.C., White, A.H. and Hoskins, B.F.: *J. Chem. Soc. Dalton Trans.*, 1369 (1972).
30. Keijzers, C.P., De Vries, H.J.M. and Van Der Avoird, A.: *Inorg. Chem.*, **11**, 1338 (1972).
31. Wickman, H.H. and Trozzolo, A.M.: *Inorg. Chem.*, **7**, 63 (1968).
32. Frank, E. and Abeledo, C.R.: *Inorg. Chem.*, **5**, 1453 (1966).
33. Ake, R.L. and Harris Loew, G.M.: *J. Chem. Phys.*, **52**, 1098 (1970).
34. De Vries, J.L.K.F., Keijzers, C.P. and De Boer, E.: *Inorg. Chem.*, **11**, 1343 (1972).
35. Wickman, H.H.: *J. Chem. Phys.*, **56**, 976 (1972).
36. Leider, H.R. and Pipkorn, D.N.: *Phys. Rev.*, **165**, 494 (1968).
37. Freeman, A.J. and Watson, R.E.: *Phys. Rev.*, **131**, 2566 (1963).
38. Karplus, M. and Pople, J.A.: *J. Chem. Phys.*, **38**, 2083 (1963).
39. Slater, J.C.: *Phys. Rev.*, **36**, 57 (1930).
40. Mulliken, R.S.: *Rev. Mod. Phys.*, **14**, 204 (1942).

Chimika Chronika, New Series, 19, 81-89(1990)

ANWENDUNG STATISTISCHER METHODEN ZUR AUSSAGEKRAFT ANALYTISCHER DATEN IM FALLE DER CHLORIERTEN KOHLENWASSERSTOFFE VON UMWELTPROBEN AUS NORDGRIECHENLAND (XANTHI).

K.OUZOUNIS

Fakultät für Ingenieurwissenschaften der Demokritos Universität Thrazien
67 100 Xanthi - Greece

(Received February 25,1988)

INHALTSÜBERSICHT

Die Ergebnisse der Korelationskoeffizienten und der berechneten Prognoseintervalle von analytischen Daten chlorierter Kohlenwasserstoffe aus Umweltproben , am Beispiel eines kleinen Datenkollektivs aus Nordgriechenland (Xanthi) , werden berichtet. Hohe korelationen wurden bei den isomeren des Hexachlorocyclohexans (a-, β-, γ-HCH) sowie bei Heptachlor und Heptachloroepoxid gefunden. Die analytische Daten und das Prognoseintervall zeigen eine niedrige Belastung dieser Umgebung.

Schlüsselwörter:Chlorierte Kohlenwasserstoffe , Korelationskoeffizienten Prognoseintervall.

EINLEITUNG

Die chlorierten Kohlenwasserstoffe sind , wegen ihre Persistenz gegenüber biotischen und abiotischen Abbau , global verteilt und Spuren einzelner Vertreter sind überall zu finden (George J.L.et al.1966). Die Aussagekraft von einzelnen Analysenergebnissen ist im allgemein gering. Dies ist eine Folge der Tatsache dass die Probennahme zwar exakt beschrieben und dokumentiert werden kann , die Probenbeschreibung jedoch unvollständing bleibt , da alle Probenparameter gar nicht erfasst werden können. Demzufolge ist eher richtig die Probennahme als Punktuellen Eingriff in einem dynamischen Umweltsystem zu betrachten , dessen Bestandteile zwar in geordneter jedoch unbekannter Weise in Wechselwirkung miteinanderstehen.

In diesem Beitrag wird versucht die im Rahmen eines Bioindikationsprogramms (Oxynos K. et al 1984) in der GSF gewonnen Erkentnisse über Aussagemöglichkeiten analytische Daten von Umweltproben (tierische Indi-

kationsorganismen) auf die analytischen Erkentnisse einer kleinen Serie von zufällig gewonnenen Umweltproben aus der Umgebung Xanthi Nordgriechenland anzuwenden. Über Herkuft , Analytik und Ergebnisse der Xanthi-Proben wurde von Ouzounis K. et al. (1985) berichtet.

Einzelne Ergebnisse der Boden und Piniennadelproben werden in Tab. 1 gegeben.

Ziel dieser Arbeit ist Modellvorstellungen , wie sie zur Umweltüberwachung mit Hilfe tierischer Indikatororganismen entwickelt wurde , anzuwenden , um aufzuzeigen ob auch mit Hilfe von stichprobenanalysen kleines Umfangs zu klaren Aussagen bezüglich der erwarteten Schadstoffkontaminationen in zukünftigen , analog gewonnenen Stichproben gelangen kann.

STATISTISCHE GRUNDLAGEN

Verteilungsform: Aus theoretischen Überlegungen (exponetielles Wachstum in biologischen Akkumulationsprozessen) ist zu erwarten dass die Konzentrationen von Schadstoffen in natürlich gewachsenen Proben nicht normalverteilt sind. Eine Annäherung zur Normalverteillung ist durch eine logarithmische (ln) Transformation zu erreichen[2].

Korrelationsparameter: Zur Erkennung von Korrelationsbeziehungen scheint es zweckmässig sowohl die linearen Regressionskoeffizienten als auch den Verteilungsfreien Spearmamsche Rho zur Betrachten.

Lineare Regression[4] : Eine Anzahl von Datenpunkten ($x_i y_i$) mit i=1,2,...n, werden einem linearen Zusammemhang (y=a+bx) angepasst. Der Korrelationskoeffizient ist:

$$R^2 = \frac{a\Sigma Yi + b\Sigma XiYi - \frac{1}{n}(\Sigma Yi)^2}{\Sigma(Yi^2) - \frac{1}{n}(\Sigma Yi)^2} \qquad (1)$$

Eine Zweidimensionale Normalverteilung der Variablen (X , Y) wird vorausgesetzt.

Spearman´s Rho[5]:Spearman´s Rang-Korrelations-Koeffizient ist ein Mass für den Zusammenhang von Rangreihen und wird als:

$$r_s = 1 - \frac{6 \sum_{i=1}^{n} Di^2}{n\,(n^2-1)} \qquad (2)$$

deffiniert.

n: Anzahl der Rangplatzpaare (Xi , Yi)

Di=Rangplatzdifferenz

$-1 \leqslant r_s \leqslant 1$

$r_s = 1$ bedeutet vollständige Übereinstimmung der Rangreihen.

$r_s = -1$ bedeutet vollständige Übereinstimmung der Rangreihen in umgekehrte Reihenfolge.

Das Prognoseintervall[6]: Ausgehend von einer normalverteilten Grundgesamtheit ,die durch eine Stichprobe von n Einzelnwerten mit den Kenndaten $\bar{x}$ (Mittelwert) und S (Standardabweichung) charakterisiert ist , wird nach dem Mittelwert ($\bar{y}$) einer zweiten Stichprobe des Umfangs m gefragt. Diese Frage führt zu dem Begriff des Prognoseintervalls , das als derjenige Konzentrationsbereich definiert ist in dem der Mittelwert ($\bar{y}$) mit einer bestimmten statistischen Sicherheit (S%) liegen soll.

$$\bar{x} - s \cdot t_{(S\%,f=n-1)} \cdot \sqrt{\frac{1}{n}+\frac{1}{m}} < \bar{y} < \bar{x} + s \cdot t_{(S\%,f=n-1)} \cdot \sqrt{\frac{1}{n}+\frac{1}{m}} \qquad (3)$$

Dabei ist t bzw $t_{(S\%,f=n-1)}$ die Schranke der t-Verteilung für f=n-1 Freiheitsgrade und S% Sicherheit zweiseitiger Fragestellung.Die Prognoseintervalle sind von Bedeutung , wenn man aus einer gegebenen Menge von Daten , auf weitere Werte , die bei zukünftigen Messungen anfallen , schliessen kann. Voraussetzung für die Anwendung des Prognoseintervalls ist die Normalverteilung der Werte oder zumindenstens eine annähernde Normalverteilung.

ERGEBNISSE UND DISKUSSION

Die statistische Auswertung der Analysendaten der aus Nordgriechenland stammenden Umweltproben[3] bezweckt einerseits die Aufdeckung von Korrelationsbeziehungen zwischen den verschiedenen Chlorkohlenwasserstoffen in einer Matrix und anderseits mit Hilfe der Prognoseintervalle

Tabelle I: Kontaminationshöhe untersuchter Boden (B) und Piniennadelproben (N) (in ng/g).

	B_1	B_2	B_3	B_4	B_5	B_6	B_7	B_9	B_{10}	B_{11}	B_{12}	B_{13}	B_{14}	B_{15}
HCB	0,3	0,06	0,9	0,06	nn	0,7	0,1	1,7	0,1	1,8	1,3	0,4	0,3	1,3
a-HCH	0,1	0,02	0,02	0,05	0,1	0,1	0,01	1,4	0,1	0,2	0,2	0,05	nn	nn
β-HCH	nn	nn	0,1	nn	nn	0,2	nn	1,0	0,2	0,3	0,1	0,05	nn	nn
γ-HCH	0,2	0,1	1,0	0,1	0,1	0,3	0,1	1,3	0,5	0,6	1,0	0,2	0,1	0,3
HC	nn	nn	nn	nn	nn	nn	nn	nn	nn	nn	nn	nn	nn	nn
HE	nn	0,2	0,02	nn	nn	nn	nn	nn	3,5	nn	nn	nn	nn	nn
Ald.	nn	nn	nn	nn	nn	nn	nn	nn	nn	nn	nn	nn	nn	nn
Diel	1,2	1,3	0,1	0,03	0,05	0,05	0,8	nn	3,3	0,3	1,0	0,2	0,1	0,03
DDE	3,0	1,2	2,4	1,0	2,3	0,7	2,0	1,2	3,3	10,0	1,8	1,7	2,6	2,5
PCB_s	0,5	0,6	0,9	0,3	nn	0,7	nn	20,0	12,5	7,0	1,3	0,3	0,4	0,3

	N_1	N_2	N_4	N_5	N_8	N_{10}	N_{11}	N_{12}	N_{13}
HCB	0,8	3,5	1,0	0,8	0,6	3,1	0,3	0,2	1,6
a-HCH	4,0	20,0	6,0	3,8	1,5	10,7	6,2	8,5	5,5
β-HCH	1,0	4,5	1,0	1,4	0,4	1,6	nn	0,2	0,5
γ-HCH	0,2	11,5	5,0	3,0	0,5	3,5	0,1	0,2	0,5
HC	0,8	5,5	1,6	0,3	0,3	1,0	0,3	0,5	0,6
HE	0,5	2,0	0,6	0,3	0,3	0,5	0,3	0,3	0,5
Ald.	1,2	3,0	1,5	0,5	0,4	0,3	3,0	0,5	1,2
Diel	0,2	1,6	0,5	0,5	0,3	1,0	0,5	0,1	0,8
DDE	1,2	2,8	1,7	1,5	0,4	7,8	4,5	0,9	2,5
PCB_s	3,3	17,0	10,5	4,0	20,0	5,8	15,4	4,0	42,0

eine Voraussage zu wagen bezüglich der bei zukünftigen Messungen zu erwartenden CKW-Konzenntrationen. Die Analysenergebnisse für die Matrix "Boden" und "Piniennadel" sind der Tabelle 1 zu entnehmen. Der Lineare und der Spearmansche Korrelationskoeffizient werden in der Tabelle 2 aufgelistet.

TABELLE II: Linearer und Spearmanscher Korrelationskoeffizient der Piniennadelproben aus Nordgriechenland.

	n	Lineare Koeffizient	S%	Spermansche Koeffizient
HCB/a-HCH	9	0,62	95	0,38
HCB/γ-HCH	9	0,64	95	0,87
HCB/β-HCH	8	0,64	95	0,82
HCB/HE	9	0,57	95	0,90
HCB/Dieldin	9	0,86	99,9	0,78
a-HCH/γ-HCH	8	0,79	99	0,32
a-HCH/β-HCH	8	0,74	95	0,27
γ-HCH/β-HCH	7	0,89	99	0,87
γ-HCH/HC	7	0,94	99,9	0,80
γ-HCH/HE	7	0,93	99,9	0,93
β-HCH/HC	8	0,88	99,9	0,67
β-HCH/HE	8	0,88	99,9	0,83
a-HCH/HC	9	0,78	99	0,52
a-HCH/HE	9	0,52	95	0,35
HC/HE	9	0,99	99,9	0,93
DDE/Dieldin	9	0,26	95	0,87
Dieldrin/PCB	9	0,09	95	0,57

n: Anzahl der Korrelierenden Paare.

S: Singnifikanter Zusammenhang auf den S%-Niveau

Aus der Tabelle 2 geht hervor dass nur vereinzeln hohe Korrelationen vorliegen und zwar auf das 95% Signifikanzniveau. Die beobachtete hohe Korrelation innerhalb der HCH-Gruppe ist durch die Anwendung des technischen Lindans leicht erklärbar. Ebenfalls verständlich ist der Zusammenhang zwischen Heptachlor und seines Metaboliten Heptachlorepoxids.

Eine interessante Korrelation , die zu Trendbeobachtungen und Überwachungszwecken geeignet scheint , ist der Zusammenhang zwischen der HCH-Gruppen und des HC/HE-paares. Bei späteren Messungen müssten ähnlich hohe Korrelationen gefunden werden , wenn unveränderliche oder sich parallel verönderte Kontamination gemessen wird. Eine Störrung der Korrelation wurde auf nicht parallele Veränderungen in der Umwelt deuten. Die fehlenden Korrelationsbeziehungen , besonders bei der Matrix "Boden" können nur mit den insgesamt sehr niedrigen Chlorkohlenwasserstoffkonzentrationen in den Matrizen "Piniennadel" und "Boden" erklärt werden. Diese lagen meistens nahe den Nachweisgrenzen des analytischen Verfahrens und waren somit mit grosser Unsicherheit behaftet.Die berechnete Prognoseintervalle der oben gennanten Matrizes werden in der Tabelle 3 aufgezeigt.

Sie werden nach einer logarithmischen Transformation der Konzentration (c→ lnc) für jeden CKW nach der Gleichung (3), für m=9 bzw m=14 Piniennadel-und Bodenproben entsprechend und S=95%, berechnet.

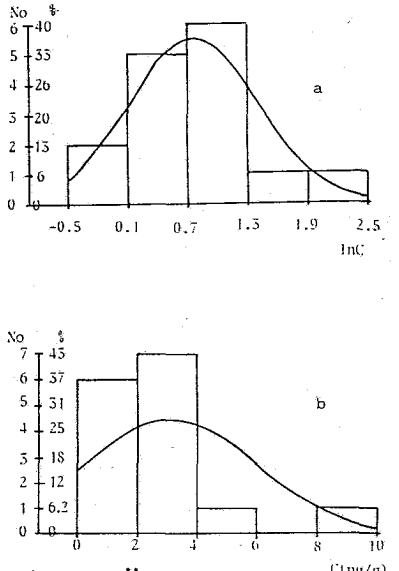

Abbildung 1: Haufigheitsverteilung für DDE in Boden
a.logarithmisch tranformierte Konzentrationen
b.Konzentrationen in ng/g

Die Brauchbakeit der logarithmischen Transformation zur Annährung der Verteilungsform der Werte an die Normalverteilung , wird in der Abbildung 1 anhand eines Beispiels demonstriert. Dass diese Transformation zweckmässig ist , wurde bei wesentlich grösserem Anzahl von Proben bei verschiedenen Matrizes gezeigt[2].

TABELLE III: Prognoseintervallgrenzen (P_{min}, P_{max}) für "Piniennadeln" und "Boden"

	Transformiente Werte (C→lnC)				Delogarothmierte Werte (C→in ng/g)			
Matrix	Piniennadel		Boden		Piniennadel		Boden	
CKW	P_{min}	P_{max}	P_{min}	P_{max}	C_{min}	C_{max}	C_{min}	C_{max}
HCB	-1,12	0,92	-2,11	0,21	0,33	2,50	0,12	1,23
a-HCH	1,01	2,53	-3,62	-1,62	2,74	12,59	0,03	0,20
β-HCH	-1,19	0,97	-2,88	-0,56	0,30	2,64	0,06	0,57
γ-HCH	-1,28	2,04	-2,15	-0,43	0,28	7,71	0,12	0,65
HC	-1,32	0,72	-	-	0,27	2,05	-	-
HE	-1,39	-0,09	-	-	0,25	0,91	-	-
Aldrin	-0,97	0,85	-	-	0,38	2,34	-	-
Dieldrin	-1,66	0,12	-2,94	0,02	0,19	1,13	0,05	1,02
DDE	-0,31	1,55	0,14	1,28	0,73	4,71	1,15	3,60
PCB s	1,33	3,19	-1,91	1,69	3,78	24,29	0,15	5,42

Die berechneten Prognoseintervallgrenzen für "Piniennadel" und "Boden" zeigen einerseits dass die jetzige Belastung mit CKW gering ist , anderseits dass zukünftige Messungen nahe an den Nachweisgrenzen der CKW zu erwarten sind. Für die Überwachungswecken ist notwendig aus dem selben Gebiet zehn Proben zu nehmen , die ln-Werte der gemessenen Konzentrationen zu bilden , den arithmetischen Mittelwert ($\bar{y}$) daraus zu berechnen und mit den in der Tabelle 3 angegebenen Intervallen zu vergleichen. Liegen diese Werte innerhalb P_{min} und P_{max} so hat auf das Signifikanzniveau von 95% keine Veränderung stattgefunden. Der begrundete Verdacht auf eine signifikante Veränderung liegt vor wenn $\bar{y}$ ausserhalb des Intervalls P_{min} bis P_{max} sich befindet. In diesem Fall ist es notwendig durch weitere

umfangreichere Messungen den angezeigten Trend zu erhärten.

Es scheint also möglich , nach der beschriebenen Vorgehenweise , anhand von zufällig gewonnenen Proben begrenzten Umfangs (n=10-20) aussagekräftige Prognoseintervalle je Matrix und Schadstoff anzugeben , mit deren Hilfe neue Messungen entweder als Konform zu den alten oder als Signifikant unterschiedlich zu klassifizieren sind.

SUMMARY

The use of statistical Methods for Estimation of Analytical Data of Environmental Samples from North Greece (Xanthi) in the case of Chlorinated Hydrocarbons.

K.OUZOUNIS

Department of Civilengineer , Dimokritio University of Thraki
67 100 Xanthi - Greece

The purpose of this paper is a. to study the reletionship between the chlorinated hydrocarbons of an indicator (soil or pine leafes) and b. the calculation of prognostic intervals and the formulation of a picture for the expected values of the future measurements.High correlation coefficients (linear and Spearman) were found in the BHC-isomers group as well as between Heptachlor and Heptachlorepoxid. The lack of correlation among the rests of the components probably comes from their very low concentrations which fall near the thresholds of the detection limits of the components (10 pg/g). The results of the chromatographic analyses and the prognostic intervals found , shows that the present level of contamination of the area is fluctuated at guite low levels.

Key words:Chlorineted hydrocarbons , correlation coefficients , prognostic intervals.

ΠΕΡΙΛΗΨΗ

Χρήση στατιστικών μεθόδων για την εκτίμηση αναλυτικών δεδομένων περιβαλλοντικών δειγμάτων από την Βόρεια Ελλάδα (Ξάνθη) η περίπτωση χλωριωμένων υδρογονανθράκων.

Στόχοι της εργασίας αυτής είναι α. η διερεύνηση συσχετίσεων μεταξύ χλωριωμένων υδρογονανθράκων ενός δείκτη (εδάφους ή φύλλων πεύκης) και β. ο υπολογισμός προγνωστικών περιοχών και διαμόρφωση μιάς εικόνας για τις αναμενόμενες μελλοντικές μετρήσεις. Βρέθηκαν υψηλοί συντελεστές συσχετισμού γραμμικού και Spearman στην ομάδα ισομερών του Εξαχλωροκυκλοεξανίου και μεταξύ Heptachlor και Heptachlorepoxid. Η έλλειψη συσχετίσεων μεταξύ των άλλων ενώσεων οφείλεται πιθανότατα στις χαμηλές συγκεντρώσεις τους , που κυμαίνονται στα όρια της ανίχνευσής τους (10pg/g). Τα αποτελέσματα των χρωματογραφικών αναλύσεων και η προγνωστική περιοχή που υπολογίσθηκε δείχνουν ότι η σημερινή επιβάρυνση της περιοχής κυμαίνεται σε χαμηλά επίπεδα.

Literatur

1.George S.L., Frear D.E.H., S.Appl. Ecol., 3 (Suppl.) 155 (1966)
2.Oxynos K., Gebefügi I., Bahadir M., Korte F., Abschlussbericht Chlorkohlenwasserstoff-Aralytik GSF/UBA: 10607023 (1984)
3.Ouzounis K., Oxynos K., Gebefügi I., Behadir M.:Chemosphere 14/10, 1571-1578, 1985.
4.Sachs L., 1982. Statistische Methoden. Springer Verlag , Berlin, Heidelberg, New York.
5.Gibbons S.D., 1971. Nonparametric Statistical Inference. New York: Mc Graw-Hill.
6.Noack S., 1980. Statistische Auswertung von Mess-und Versuchsdaten mit Taschenrechner und Tischcomputer , Walter de Gruyter , Berlin , New York.

Chimika Chronika, New Series, 19, 91-104(1990)

STUDY OF THE INTERACTION OF *Gerardia savaglia* MANNOSE-SPECIFIC LECTIN, WITH RECEPTORS ON P3X-63 MOUSE MYELOMA CELLS

M.ČUPERLOVIĆ[1], LJ.HAJDUKOVIĆ[1], D.BUGARSKI[1], S.POZNANOVIĆ[2], Z.KLJAJIĆ[3] and M.J.GAŠIĆ[4]

[1]*Institute of Endocrinology, Immunology and Nutrition, INEP, Zemun,*
[2]*Institute of Chemistry, Technology and Metallurgy, Belgrade,*
[3]*Institute for Marine Biology, Kotor, and*
[4]*Department of Chemistry, University of Belgrade, Yugoslavia*

(Received March 26, 1990)

SUMMARY

Murine BALB/c myeloma cells (clone P3Y-63.Ag8 653) were used to study binding kinetics of *Gerardia savaglia* lectin. The fluorescein isothiocyanate labelled lectin stained the surface of these cells forming a speckled-type pattern. Using iodinated *Gerardia* lectin, a dose-response binding curve was obtained with a tendency towards saturation of binding sites at lectin concentration of 1.5 nM/10^6 cells. The constructed Scatchard plot was consistent with a complex system containing one ligand and two classes of binding sites. Binding of iodinated *Gerardia* lectin to mouse myeloma cells was inhibitable by mannose or by unlabelled *Gerardia* lectin. Another mannose-specific lectin, concanvalin A, also displaced the iodinated *Gerardia* lectin to the level of 56% of the maximal binding, while the addition of *Lens culinaris* lectin had an opposite effect and increased binding of ^{125}I-GSL to nearly 200% of the initial value. This positive cooperativity is consistent with receptor rearrangements and the accessibility of new ligands for *Gerardia* lectin induced by the exposure of mouse myeloma cells to *Lens culinaris* lectin.

KEY WORDS

Gerardia savaglia lectin - Binding kinetics - Positive and negative cooperativity - Mouse myeloma cells

INTRODUCTION

The coral *Gerardia savaglia* contains a lectin which was recently isolated and characterised[1]. The *Gerardia savaglia* lectin (GSL) is a glycoprotein M_r 32 kD, composed of two polypeptide chains. It shows specificity for D-mannose, as determined by haemagglutination-inhibition, requires Ca^{2+} ions for full activity and precipitates erythrocytes from humans (A,B,O), sheep, rabbit and carp. The lectin exhibited some peculiar features toward mammalian cells[2].

A presumably B-lymphocyte activator, it caused proliferative response of spleen cells only in the presence of some other B-lymphocyte mitogens as lipopolysaccharide, but neither alone nor in combination with T-lymphocyte mitogens like Concanavalin A. It was also found that GSL binds to plasma and nuclear membranes of various cells, forming a characteristic speckled-type of patterns[3]. Additionally, binding of the lectin to nuclear envelope of isolated nuclei had inhibitory effect on mRNA efflux from nuclei and on NTPase activity[2].

It was here attempted to investigate interaction of this lectin with BALB/c myeloma cell line by a quantitative binding study. The applied clone P3X-63.Ag8 653[4] is rountinely used for fusion with antibody-forming cells to obtain hybrid cell lines producing monoclonal antibodies, and therefore represents a constantly available pool of cells for binding studies.

EXPERIMENTAL

Materials

Gerardia savaglia lectin was isolated from the anthozoan *Gerardia savaglia* (Bert.; Hexacorallia, Gerardiidae) which was collected in the bay of Kotor, processed as previously described[2,3], and finally purified on Sepharose 6B-mannose affinity column. Concanavalin A (Con A) and *Lens culinaris* (LCA) lectin were prepared according to described methods[5,6].

Iodobeads were purchased from Pierce, ^{125}I(NaI) carrier-free from Amersham International, Dulbecco's modified eagle's medium (DMEM) from Gibco, and bovine serum albumin (BSA), foetal bovine serum (FBS), sodium pyruvate, L-glutamine, HEPES, fluorescein isothiocyanate (FITC) (isomer 1) and D-mannose were from Sigma Chemical Co. These and all other chemicals applied were p.a. grade.

Conjugation of GSL with FITC and lectin fluorescence microscopy

Lectin was conjugated with FITC according to the procedure used for immunoglobulin labelling[7] and subsequently purified by gel filtration (Sephadex G-25). This preparation (F/P=2) was used for staining of P3X-63.Ag8 653 cells which was performed by incubation of 10^5 cells in 25 µl of GSL-FITC solution (lectin concentration 40 µg/ml) at 4°C for 30 min. The stained and rinsed cells were analysed under an Option, Standard IFD microscope (Carl Zeiss) equipped with epifluorescence optics. The specificity of binding was proved by complete inhibition of staining after the addition of 200 mM mannose into the incubation medium.

Cell culture

The P3X-63.Ag8 653 myeloma cells were grown in DMEM medium supplemented with 10% FBS, 2 mM L-glutamine, 100 mM HEPES and 1 mM sodium pyruvate at 37°C in a humidified atmosphere of 7% CO_2 in-air. Cells were mainained in continuous culture not exceeding the density of $2.5x10^5$ cells/ml. The cell viability was determined with trypanblue and was greater than 95% at the time of collecting the cells.

Iodination of Gerardia savaglia lectin

GSL was labelled using iodobeads. Briefly, eight iodobeads were soaked in 400 µl of 20 mM Tris-HCl buffer, pH 7.2, containing 150 mM NaCl and 1 mM Ca^{2+}, Mg^{2+} and Mn^{2+} (Tris buffered saline - TBS). Upon the addition of 10 µl $Na^{125}I$ (2 mCi), the reaction mixture was incubated

for five minutes with occasional shaking, followed by the addition of 1 ml lectin solution containing 2 mg of GSL and further 15-min incubation. Eventually, labelled protein was separated on Sephadex G-25 column. The specific activity of the obtained preparation was 10^7 Bq/mg.

The procedure for GSL iodination did not affect its agglutinating activity for rabbit erythrocytes, as determined by haemagglutination assay before and after iodination.

Binding assay

Gerardia lectin was dissolved in TBS supplemented with 0,5% BSA and filtered through a 0.22 /um sterile filter. Initial lectin concentration was 1 mg/ml. From this solution, 12 dilutions were made ranging from 10-750 /ug GSL/ml.

Iodinated GSL was also diluted by TBS to the concentration of 10 /ug GSL or 5.10^6 cpm/ml. P3X-63 cells were resuspended in TBS to the concentration of 10^7 cells/ml or as specified.

Binding assays were performed in polystyrene test tubes (12x75 mm) which were preincubated overnight with 0.5 ml 1% BSA solution and rinsed.

Equal volumes (100 /ul) of GSL dilutions, solutions of ^{125}I-GSL and of cell suspension were added to test tubes and the assay mixture was incubated at room temperature for one hour and shaken occasionally. Supernatant fluid was separated by brief centrifugation (1000 rpm, 5 min) and 50 /ul aliquots were taken for counting. Pellets were rinsed three times in TBS and the bound activity counted using a Gammachem 4800 counter (Biodata).

The nonspecific binding of ^{125}I-GSL was determined in the presence of 200 mM D-mannose under the same experimental conditions. It amounted to approximately 10% and was substracted from the total bound activity. All incubations were made in triplicate.

RESULTS

The binding of *Gerardia* lectin to P3X-63.Ag8 653 cells was visualised by staining the cells with fluorescein-labelled GSL. The applied lectin concentration did not produce a noticeable agglutination of the cells, but a speckled-type of staining pattern was evident (Fig. 1).

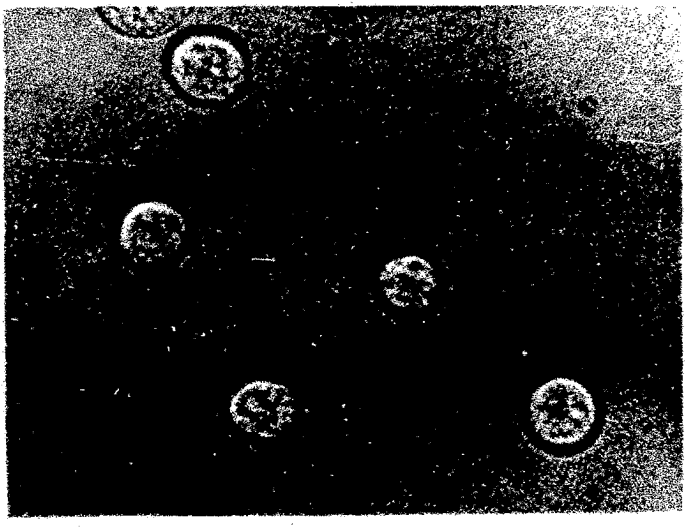

FIG. 1: *Single direct immunofluorescence microscopy of P3X-63.Ag8 653 cells with fluorescein isothiocyanate-labelled Gerardia lectin. magnification:* x 252.

The addition of 100 mM D-mannose completely abolished the fluorescence. Binding characteristics of *Gerardia* lectin were more closely investigated by means of ^{125}I-labelled lectin. The influence of cell density on ^{125}I-GSL binding is illustrated in Fig. 2A. Lectin binding increased with the increase of cell number, so that cell density for subsequent studies was adjusted to the convenient 10^6 cells per total assay volume of 300 µl.

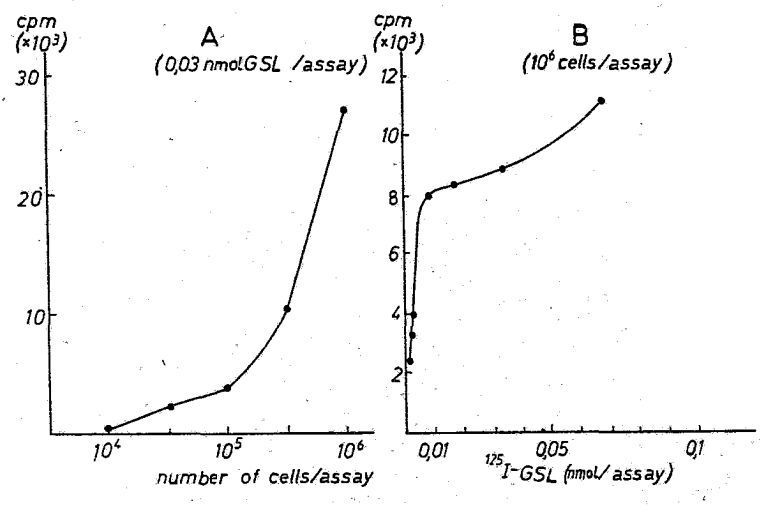

FIG. 2: *Specific binding ^{125}I-GSL to P3X-63.Ag8 653 cells as a function of cell density (A) and lectin concentration (B). Assay volume 300 µl, incubation time 60 min at room temperature.*

A dose-response curve for GSL binding at very low lectin concentrations (0.001-0.067 nmol/assay) is shown in Fig. 2B.

For the study of specific binding at a higher saturation of binding sites, labelled GSL was combined with untreated lectin to acquire total lectin concentration of reaction mixture ranging from 0.03-1.6 nmol/assay. The obtained pattern (Fig. 3) was that of a saturable specific binding with the indication of saturation of binding sites at the highest concentrations of the examined lectin. This binding was analysed by Scatchard plot (Fig. 4). The obtained curvilinear graph indicated a complex system containing one ligand and more, possibly two, classes of binding parameters[8], it could be calculated that the number of high affinity binding sites, saturable at low lectin concentrations, amounted to approximately 10^6 per cell, while that of low affinity binding sites was one order of magnitude greater. The corresponding affinity constants would be near $10^{10}M^{-1}$ for low lectin concentrations and high-affinity

bindings sites, and about 20 times lower for higher lectin concentrations near saturation values.

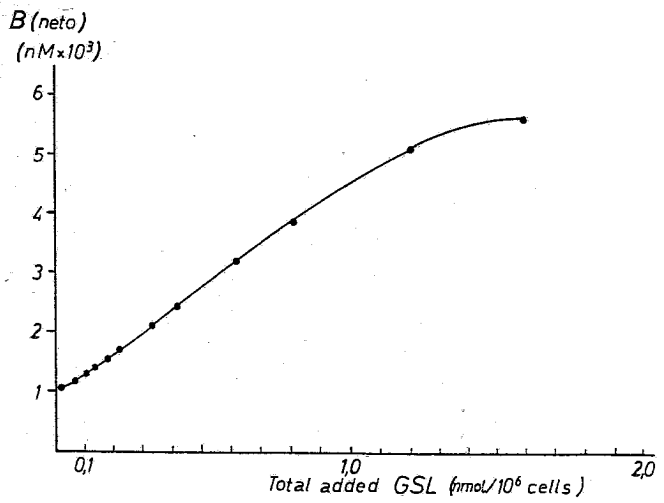

FIG. 3: *Binding (B) of GSL to P3X-63.Ag8 653 cells. Cells were incubated with GSL + ^{125}I-GSL. Assay conditions as in Fig. 2.*

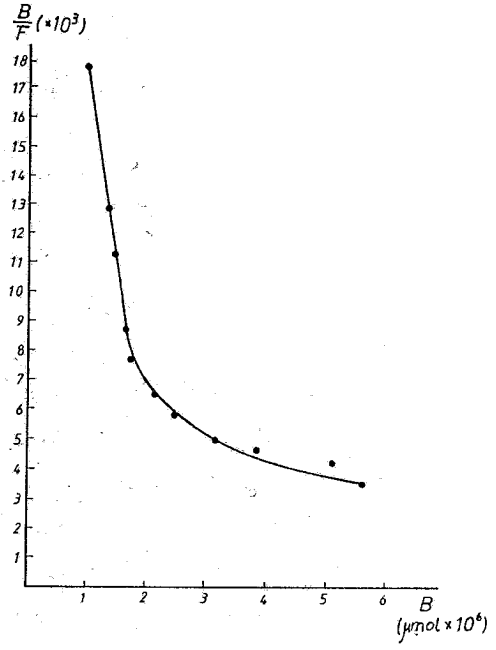

FIG. 4: *Scatchard plot of GSL binding to P3X-63.Ag8 653 cells. 10^6 cells per 300 µl of incubation medium. Lectin concentrations as in Fig. 3.*

The interaction of GSL with the sites present at the surface of P3X-63 cells was mannose-inhibitable. Bound ^{125}I-GSL was also efficiently displaced by higher concentrations of untreated *Gerardia* lectin, and the obtained displacement curve had smooth sigmoidal shape (Fig. 5).

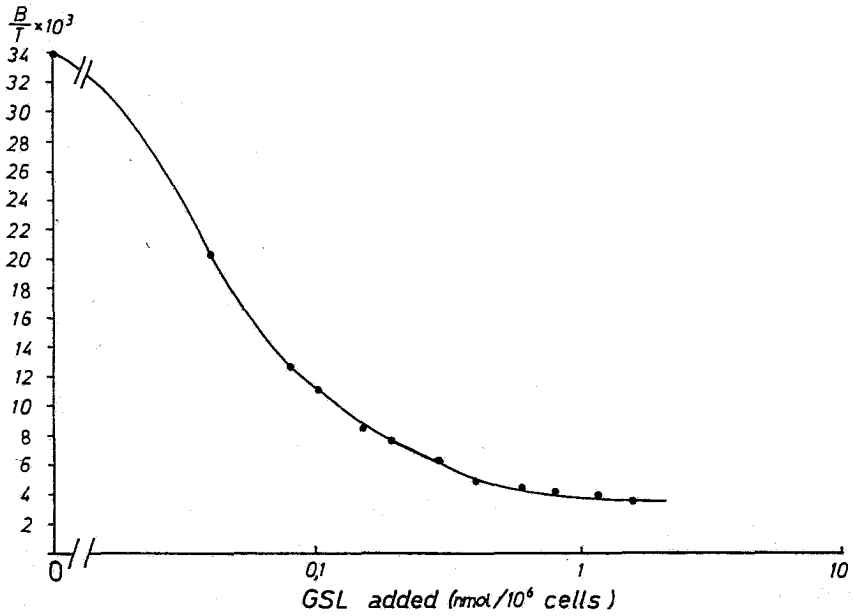

FIG. 5: *Displacement of ^{125}I-GSL by increasing doses of GSL. ^{125}I-GSL concentration was constant and amounted to 0.03 nmol/10^6 cells.*

Competition for binding of GSL with other mannose-specific lectins was also investigated. ^{125}I-GSL was combined with GSL, Con A or LCA and then used for binding assay, as described. While the concentration of ^{125}I-GSL was constant (2 μg/assay), each of the added lectins was tested in four serial dilutions from 135-16.9 μg/assay. All four concentrations corresponded to the level of inhibitory lectin that gave a lower plateau of GSL-displacement curve. Accordingly, the addition of GSL reduced binding of ^{125}I-GSL to 26% on average of the value obtained with iodinated lectin only (Fig. 6). The addition of Con A also had an inhibitory effect and reduced ^{125}I-GSL binding to 56% on average of

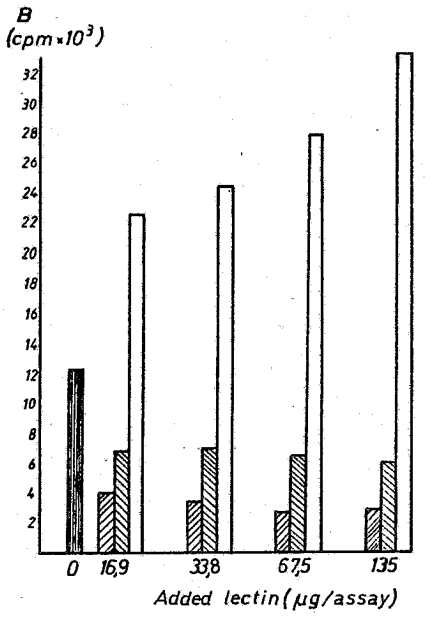

FIG. 6: *Effects of the added lectin GSL* ▨, *Con A* ▧, *and LCA* □ *on the binding of* ^{125}*I-GSL to P3X-63.Ag8 653 cells. Assay conditions as described in Fig. 2.* ^{125}*I-GSL concentration was 2 µg/tube.*

maximal values. Inhibitory effects of all four dilutions of these two lectins (GSL and Con A) were similar, with insignificant increase of ^{125}I-binding at serial dilutions of the added lectins. The addition of LCA, however, had a strikingly different effect on ^{125}I-GSL binding. As shown in Fig. 6, after combining ^{125}I-GSL and LCA, binding of the iodinated lectin was increased to 164-244% of starting value, and was directly proportional to the concentration of the added LCA.

DISCUSSION

In the present study, binding characteristics of *Gerardia savaglia* lectin were examined using a mouse myeloma cell line. This clone of B lymphocytes does not express immunoglobulin-heavy or light chains and is often used for fusion with antibody-forming cells. P3X-63.Ag 8 653

cells can be successfully maintained as a continuous culture under standard conditions which represents a convenient model for binding experiments. GSL binds to the surface of these cells forming a characteristic speckled-type pattern. Similar staining patterns were obtained with two other mannose-specific lectins (Con A-FITC and LCA-FITC) when incubated with mouse myeloma cells under the same conditions (results not presented in this report). However, in spite of this superficial similarity, lectin isolated from the coral *Gerardia savaglia* has some peculiar characteristics. Namely, most lectins from lower eukaryotes are D-galactose-specific, but the *Gerardia* lectin recognises D-mannose and, with a 50-fold lower affinity, D-glucose[2]. This monosaccharide specificity is comparable with the specificity of Con A and, in addition, both lectins require Ca^{2+} for full activity. However, the affinity of GSL for more complex structures appeared to be different from that of Con A. Thus, haemagglutination-inhibition experiments indicated that D-Manα1 $\longrightarrow$ 2D-Man disaccharides are most powerful inhibitors of GSL activity. When used as a ligand in lectin affinity chromatography, GSL was incapable to retain choriogonadotrophin, alfa-fetoprotein and several other glycoproteins that have complex N-linked oligosaccharide chains containing 3-mannosyl core (our unpublished data). All these glycoproteins were completely or partially retained by Con A and LCA when these lectins were used as ligands[9]. The histochemical examination of various tissue sections with GSL-FITC conjugate gave distinct staining patterns[3]. More detailed investigations showed that, *in vitro*, lectin binds to a glycoprotein present in the nucelar envelope and such binding had an inhibitory effect on mRNA translocation system of isolated nuclei from CV-1 monkey kidney cells[2].

The presented results are consistent with a complex pattern of receptors for GSL exposed on the surface of mouse myeloma cells. This type of binding kinetics and non-linear Scatchard plots had also been observed for a number of other lectins and cells[10,11], and were explained

by the multiplicity of binding sites with different affinities, or by negative cooperative site-site interactions among a homogenous population of receptors which have high affinity when unoccupied, but switch to a low-affinity conformation as occupancy increases. In most equilibrium or kinetic experiments the negative cooperativity model can not be distinguished from that of low and high-affinity receptors, and our system is not the exception.

The whole population of receptors for GSL on P3X-63 cells approached saturation at lectin concentration of 40-50 $\mu g/10^6$ cells. It can be argued, though, that under the experimental conditions used, some amount of lectin was internalised or degraded and that such effects influenced saturability of GSL binding. This possibility will be more closely examined, but the fact that GSL binding is abolished by a specific haptenic sugar indicated that it was predominantly a cell surface-mediated phenomenon.

The interaction of GSL with all sites present at the surface of P3X-63 cells is mannose-inhibitable. Labelled ligand is also displaced by unlabelled GSL, giving a displacement curve of smooth sigmoidal shape that reached lower plateau when GSL/^{125}I-GSL molar ratio exceeded 10.

The other two examined mannose-specific lectins had very pronounced effects on negative (Con A) and positive (LCA) cooperativity of GSL binding to P3X-63 cells. Therefore, the addition of Con A to ^{125}I-GSL in molar ratios corresponding to a lower plateau of the GSL displacement curve resulted in the inhibition of ^{125}I-GSL binding which was comparable to inhibition obtained by the addition of unlabelled GSL. This would tentatively imply a competition between GSL and Con A for the same binding sites which would fulfil the binding requirements of both lectins, i.e. contain 3-Man-core and exposed mannose (or preferentially 2-Man) residues.

The effect of another mannose-specific lectin, LCA, on ^{125}I-GSL binding to P3X-63 cells indicated a more complex relationship. The

addition of LCA to ^{125}I-GSL resulted in tremendous increase of ^{125}I-GSL binding to P3X-63 cells which was positively dependent on LCA concentration within the range of 5 to 40 LCA/GSL molar ratio. An explantion of this effect should be sought in the classical concept of positive cooperativity of binding, which connects positive cooperativity with the exposure of new binding sites or with increased affinity of existing sites. In many cells, exposure to lectins creates cytoskeletal rearrangements of receptors which can result in higher local density of receptors or exposure of next binding sites and their increased accessibility to another ligand. Cross-linking and reorganization of headgroups were also envisaged as possible cause of positive cooperativity in a model membrane treated with lectins[12]. The mitogenic effect of GSL on murine spleen lymphocytes can be expressed only when lectin is applied in combination with another mitogen[2], which also suggests that spatial rearrangement in the plane of the plasma membrane is necessary for the accessibility of new ligands and maximal binding of *Gerardia* lectin, followed by mitogenic response of the cells. Other explanations of the obtained effects of LCA on GSL binding are also possible, such as bridging of LCA between cell membrane glycoproteins ang GSL, or penetration of *Gerardia* lectin through the cell membrane after its exposure to LCA. Studies to elucidate some of these possibilities and relationships of mannose-specific lectins and receptors on the surface of P3X-63.Ag 8 653 cells are in progress.

Acknowledgment. This work was supported by the Serbian Republic Research Fund.

REFERENCES

1. Kljajić, Z., *Occurrence, isolation, and characterization of some lectins of marine invertebrates*, Ph. D. Thesis, University of Belgrade (1986).
2. Kljajić, Z., Schröder, H.C., Rottmann, M., Čuperlović, M., Movsesijan, M., Uhlenbruck, G., Gašić, M.J., Zahn, R.K. and Müller, W.E.G., *Eur. J. Biochem* 169, 97 (1987).

3. Kljajić, Z., Gašić, M.J., Čuperlović, M., Movsesijan, M., Sladić, D., Zahn, R.K. and Müller, W.E.G., *INTERLEC 9*, Cambridge, England (1987).
4. Karney, J.F., Radbruch, A., Leisegang, B. and Rajewsky, K., *J. Immunol.* 124, 1548 (1979).
5. Agrawal, B.B.L. and Goldstein, I.J., *Concanavalin A, the jack bean (Canavalia ensiformis) phytohemagglutinin,* in Ginsburg 5th ed: Methods in Enzymology, Vol. 28, part B, pp 313-318, Academic Press, New York (1972).
6. Sage, J.H. and Green, R.W., *Common lentil (Lens culinaris) phytohaemagglutinin,* in Ginsburg 5th ed: Methods in Enzymology, Vol. 28, part B, pp 332-339, Academic Press, New York (1972).
7. The, T.H. and Feltcamp, T.E.W., *Immunology* 18, 865 (1970).
8. Benkirane, M., Bon, D., Bellot, F., Prince, P., Massoun, J., Carayon, P. and Delori, P., *J. Immunol. Methods,* 98, 173 (1987).
9. Nikolić, A., Čuperlović, M., Hajduković, Lj. and Janković, M., 19th FEBS meeting, Rome, (1989).
10. Prigent, M. and Boquet, P., *Biochim. Biophys. Acta.* 717, 445 (1982).
11. Čuperlović, M., Cerović, G. and Milošević, Z., *Binding of PHA, WGA and SBA to the surface of rat intestinal epithelial cells in vitro,* in Bog-Hansen, T., C., and van Dressche, E., Lectins, Vol. V, pp 493--498, Walter de Gruyter & co., Berlin, New York (1986).
12. Ketis, N.V. and Grant, C.W.M., *Biochim. Biophys. Acta* 689, 194 (1982).

Chimika Chronika, New Series, 19, 105-109(1990)

SHORT PAPER

SYNTHESE DE QUELQUES DERIVES AMINES ISOSTERES DU BENZOMORPHANE

N.KOLOCOURIS et P.MARACOS

Université d' Athènes, Laboratoire de Pharmacie Chimique 104, rue Solonos, Athènes 10680 Grèce.

Received : March 30.1988

Keywords : Central analgesics / methanobenzocyclooctenamines, synthesis of

INTRODUCTION

Les derivés du benzomorphane (méthanobenzazocine) 1 constituent une catégorie d'analgésiques centraux. L'intérêt de ce groupe de composés, qui a donné des médicaments intéressants (phénazocine, pentazocine e.t.c.) et dont la recherche continue intensement[1,2,3], se situe au fait que certains de ces membres présentent une séparation complète de l'activité analgésique de l'accoutumance[4].

Dans les molécules des benzomorphanes l'atome de l'azote participe au cycle azocinique. Le présent mémoire décrit la synthèse de quelques méthanobenzocycloocténamines 2 qui sont isostères aux benzomorphanes et ont l'originalité de posséder l'atome de l'azote en position exocyclique (Schéma I).

La synthèse de dérivés aminés 2 a été réalisée, suivant le schéma II, par l'action d'un dérivé dihalogéné[5,6] sur les

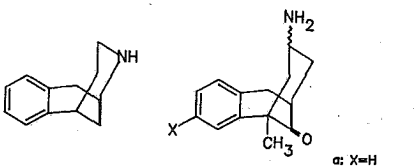

1 2

a: X=H
b: X=OCH3

Schéma I

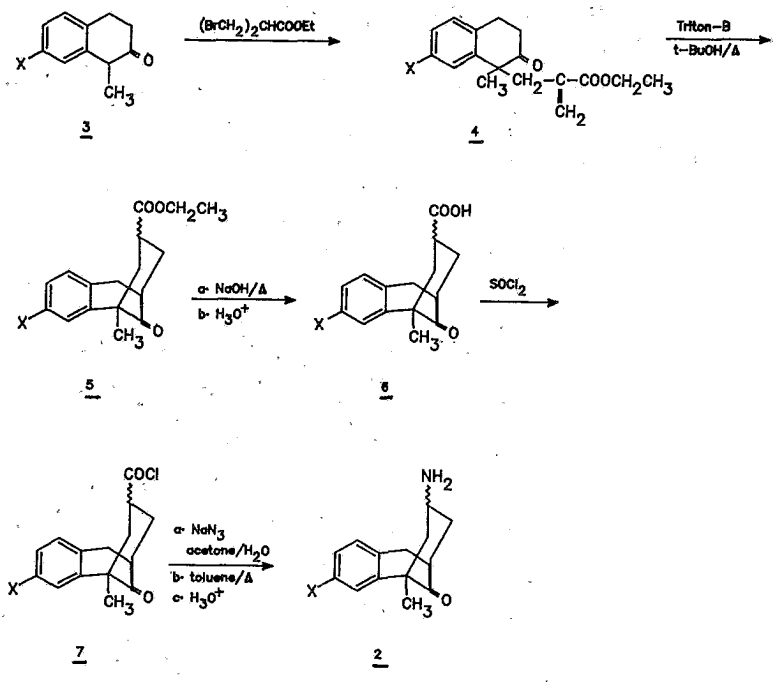

Schéma II

méthyl-1-tétralones-2 [7,8,9]. Plus précisement, nous faisons réagir le bis(bromométhyl)acétate d'éthyle[10] avec les méthyl--1-tétralones-2 en présence d'hydrure de sodium; ils se forment les cétoesters insaturés 4, qui par chauffage dans le t-BuOH en présence de Triton-B, subissent une cyclisation intramoléculaire du type Michael et fournissent les cétoesters polycycliques 5; la saponification de ces cétoesters donne les cétoacides 6 correspondants, qui par chauffage avec le chlorure de thionyle sont transformés en chlorures 7. L'application de la réaction de Curtius sur ces derniers permet d'aboutir aux aminocétones 2.

L'étude au RMN des cétoacides 6 et des amines 2 nous amène à la conclusion que ces composés sont des mélanges des diastéréoïsomères (double absorption du groupement méthyle en position 5)

Partie Expérimentale

Les points de fusion ont été pris dans un appareil de Büchi et ne sont pas corrigés. Les microanalyses ont été effectuées par le Service Centrale de Microanalyse du C.N.R.S. et sont conformes aux valeurs théoriques à ±0,4 % .Les spectres RMN-^{1}H ont été enregistrés sur un appareil Varian-FT-80A en utilisant le $CDCl_3$ comme solvant et la TMS comme référence interne. Les spectres IR ont été enregistrés sur un spectrophotomètre Perkin-Elmer 177.

Hexahydro-5,6,7,8,9,10,méthoxy-3,méthyl-5,oxo-11,méthano-5,9-benzocyclooctènecarboxylate d'éthyle-7. 5b. (X=CH_3O).

Dans une solution de 8,3g (0,043 mole) de méthoxy-7, méthyl-1,tétralone-2 dans 40ml de DMF anhydre, on ajoute sous atmosphère d'azote, agitation et refroidissement,2g(0,046mole) d'hydrure de sodium à 55% dans l'huile minérale préalablement lavé dans du benzène anhydre. On agite pendant 20min à la température ambiante, puis sous refroidissement, ajoute en une seule fois 12,6g (0,046 mole) de bis(bromométhyl)acétate d'éthyle. Après deux heures d'agitation à la température ambiante, on refroidit de nouveau et y ajoute par petites quantités 2g(0,046 mole) d'hydrure de sodium à 55%. On chauffe vers 120°C pendant 2h (toujours sous courant d'azote). Après refroidissement le mélange est versé dans un excès d'eau et de glace et extrait à l'éther. La couche éthérée est lavée à l'eau, sechée sur Na_2SO_4 et évaporée. Le résidu est distillé sous pression réduite et on recueille la fraction liquide qui passe vers 120-170°C/0,03mmHg, soit 12,2g. Cette fraction contient surtoût l'ester insaturé liquide 4b(accompagné parfois par de petites quantités d'ester tricyclique 5b) IR(film) cm^{-1}: ν(C=O) cétone et ester (mal séparés) 1710, ν(C=C) 1620, ^{1}H-RMN ($CDCl_3$) δ ppm: 1,06-1,23(t,3H,$\underline{CH_3}CH_2O$) 1,44(s,3H,$\underline{CH_3}$-1) 2,47-3,25(m,6H,2xCH_2 cyclohexaniques, $\underline{CH_2}$-C=CH_2) 3.78(s,3H,$\underline{CH_3}O$) 3.84-4.00(q,2H,O$\underline{CH_2}CH_3$) 5.35(d,1H,Jgem~ 0,8Hz,=CH) 6,04(d,1H,

Jgem~0,8Hz,=CH) 6,57-7,08(m, 3H, aromatiques).

Le produit distillé est mélangé avec 30ml de t-BuOH et 2ml de Triton-B(en solution 40% dans le méthanol) et chauffé au bain-marie pendant 8h. Le mélange est versé dans un excès d'eau et de glace et extrait à l'éther. La couche éthérée est lavée à l'eau, séchée sur Na_2SO_4 et évaporée. Le résidu cristallise dans le n-pentane.

Rdt : 45% par rapport à la tétralone, F=109°C (éther) IR(nujol)cm^{-1}: ν(C=O) cétone 1710, ν(C=O) ester 1700, ^{1}H-RMN ($CDCl_3$) δppm:0,88-1,27(t,3H,$CH_2\underline{CH_3}$) 1,45(s,3H,CH_3-5) 1,77-3,65 (m,10H,H-6,H-7,H-8,H-9,H-10,-$CO_2\underline{CH_2}$) 3,77(s,3H,$\underline{CH_3}O$) 6,43-7,10 (m,3H,aromatiques).Analyse : ($C_{18}H_{22}O_4$) % Calc.:C=71,49 H=7,35 % Tr.:C=71,52 H=7,31.

En utilisant la même méthode nous avons synthétisé le cétoester 5a (X=H) [F:103°C (éther) Rdt:42%] dont la structure est confirmée par son analyse élémentaire et ses donées spectrales qui sont proches à celles de l'ester 5b.

Acide hexahydro-5,6,7,8,9,10, méthoxy-3, méthyl-5, oxo-11, méthano-5,9-benzocycloocténecarboxylique-7. 6b.

La saponification du cétoester 5b (4,6g) avec une solution de soude (7g) dans 50ml d'éthanol 95° pendant 8h à 60°C, suivie d'évaporation de l'éthanol en excès, addition de l'eau et acidification avec de l'acide chlorhydrique dilué, fournit le cétoacide 4b qui cristallise dans un mélange éther-n-pentane. Rdt:92%, F:188°C, IR(nujol)cm^{-1}: ν(C=O) carboxyle 1680, ν(C=O) cétone 1710, ^{1}H-RMN ($CDCl_3$) δppm : 1,43 (~s,3H,$\underline{CH_3}$) 1,92-2,83 (m,6H,H-8,H-6,H-7,H-9) 3,22-3,66(d,2H,H-10) 3,71(s,3H,$\underline{CH_3}O$) 6,50-6,85(m,3H,aromatiques) 10,67(s,1H,CO_2H,disparaît avec D_2O) Analyse : ($C_{16}H_{18}O_4$) %Calc.:C=70,12 H=6,51 %Tr.:C=70,07 H=6,56

En travaillant de la même façon nous avons synthétisé le cétoacide 6a (X=H) [F:165°C (éthanol 95°), Rdt:94%] dont la structure est confirmée par son analyse élémentaire et ses données spectrales qui sont proches à celles de l'acide 6b.

Hexahydro-5,6,7,8,9,10, méthoxy-3, méthyl-5, oxo-11, méthano-5,9-benzocycloocténamine-7, HCl. 2b.

5g (0,0182 mole) de cétoacide 6b sont transformés en chlorure par chauffage avec 13ml de $SOCl_2$ vers 70°-80°C. Après élimination du $SOCl_2$ sous pression réduite à l'aide aussi de benzène anhydre, le résidu est dissous dans 30ml d'acétone anhydre. Cette solution acétonique est ajoutée très lentement (en 6 min), sous vive agitation et refroidissement, dans une solution de 5,91g (0,091 mole) de NaN_3 dans 25ml d'eau. Le mélange est agité pendant 15min vers 0°C et pendant 20min à la température ambiante, puis extrait au benzène. La couche benzénique est laveée à l'eau et séchée très bien sur Na_2SO_4. Après avoir évaporé le benzène sous pression réduite, on ajoute du toluène anhydre et chauffe vers 95°-100°C. Après décomposition de l'azide et refroidissement, on ajoute 5ml d'acide chlorhydrique 1/1 et le mélange est agité fortement pendant 10min. On évapore le solvant et cristallise le résidu dans l'éther. Rdt par rapport au cétoacide 6b : 78%, F:201-202°C (éthanol.abs.-éther), IR(nujol)cm^{-1}: ν(C=O) cétone 1710, ^{1}H-RMN (DMSO- dδ) δppm: 1,33(~s,3H,CH_3) 1,74-2,62(m,5H,H-6,H-8,H-9) 2,67-2,88 (m,1H,H-7) 2,91-3,24(~d,2H,H-10) 6,75-7,17(m,3H,aromatiques) 8,26(br.s,3H,NH_3^+,disparaît avec D_2O). Analyse : ($C_{15}H_{20}NO_2Cl$) %Calc.:C=63,94 H=7,10 N=4,97 Cl=12,61 %Tr.:C=64,07 H=7,14 N=4,91 Cl=12,34.

En utilisant la même méthode nous avons préparé le chlorhydrate de l'amine 2a (X=H) F:238°C (déc.) Rdt:65% dont la structure est confirmée par son analyse élémentaire et ses données spectrales qui sont proches à celles de l'amine 2b.

SOMMAIRE

Nous décrivons la synthèse de dérivés aminés isostères du benzomorphane, en faisant réagir les méthyl-1-tétralones-2 avec le bis (bromométhyl) acétate d'éthyle et transformation du groupement ester du cétoester intermédiaire en groupement amine avec la réaction du Curtius.

Chimika Chronika, New Series, 19, 111-118(1990)

NOTE

IMPROVED PROCEDURE FOR THE FLUOROMETRIC DETERMINATION OF SELENIUM IN BIOLOGICAL MATERIALS

A.AYIANNIDIS*and A.VOULGAROPOULOS**

* *Chemistry Lab. of Veterinary Dept. Aristotelian University of Thessaloniki.*

** *Analytical Chemistry Lab. of Chemistry Dept. Aristotelian University of Thessaloniki, 540 06 Thessaloniki, GREECE.*

(Received 20-11-1989)

INTRODUCTION

The biological role of the selenium is well documented[1,2], so that its determination in biological materials to become, already of long time ago, a necessity for the Clinical Pathology of the Veterinary Dept. at the University of Thessaloniki.

However, applying[3,4] methods previously published[5-11], it was noticed that the determination of selenium suffers mainly with respect to the reproducibility. Thus, it was thought, that it could be formulated a new analytical scheme by modification and combination of certain stages used in the above methods.

Key words: Selenium; fluorometric determination; wet digestion; biological materials.

EXPERIMENTAL

Apparatus

1. Fluorometer. A Zeiss fluorometer, model PMQ II was used throughout the work. The excitation source was a mercury lamp of St 41 model and the cuvette receiver of ZEM 4 model in a B arrangement. 365 nm was chosen as excitation wavelength, while 520 nm as emission using in combination an excitation filter F 56.

2. Thermostated digestion shelf. The shelf was equipped with a contact thermometer allowing variation $\pm 2^{o}C$, as well as with a heat regulator producing a rate of temperature increase of about $75^{o}C/h$.

Reagents

All reagents used were of E.Merck of p.a. grade, except if it isotherwise stated in the text, while the "pure" water was obtained by single distillation followed by de-ionization.

1. Digestion acid mixture. This mixture was prepared of concentrated nitric, perchloric and sulfuric acids in a volume ratio 2+2+1 respectively. 2. Cresol red indicator. 0.1g cresol red was dissolved in 10 ml of alkaline warm water and the resulted solution was diluted up to 500 ml. 3. Ammonium hydroxide. A 7M solution was prepared by dilution of about 535 ml ammonium hydroxide 25%, d=0.91, up to 1l. 4. Disodium ethylenedinitrilotetracetate dihydrate (EDTA, Titriplex III). A solution of 1.5% was used. 5. Sulfuric acid solution. A solution of 14% was used. 6. Cyclohexane. The cyclohexane was distilled before its use in a glass apparatus. 7. 2,3-Diaminonaphthalene (DAN) solution. 0.1 g of 99% purity DAN, supplied from Aldrich Co., was dissolved in 10 ml of 14% sulfuric acid solution (reagent 5) The dissolution was taking place under continuous and vigorous stirring for about 2 min in a volumetric cylinder of 25 ml closed by its grounded stopper. In the same cylinder, 10 ml of cyclohexane (reagent 6) were added;then the content was stirred again for about 2 min and was left to stay for about 10 min. The useful aqueous layer can be taken easily by a piston pipette. The solution and its exctraction were made just before the use of the reagent. 8. Stock selenium solution of about 1 g/l as selenites. 0.3513 g selenium dioxide was dissolved in about 50 ml water and after the dissolution was completed, it was diluted up to 250 ml. The latter was titrated iodometrically[12] to determine accurately its concentration; it was remade monthly. In the present work the selenium dioxide was purified by sublimation[13] before its use. Work standard selenium solutions of 10, 25 and 50 µg/l were prepared by successive dilutions of the above stock solution and they were kept in the darkness; they were remade weekly.

Procedure

1. A weighed or pipetted sample (e.g. 2 ml whole blood, 1 g of alfalfa meal or of liver wet tissue) as well as certain volume of a standard solution are placed respectively in Kjeldahl flasks (usually of 100 ml). It is noted that especially biological samples should not contain more than 300 ng of selenium and that those parts of the sample stuck on the flask neck should be transferred to the bulb by means of water (usually 2-3 ml). The

determination of the moisture in solid samples is carried out separately according to established thermal procedures. 2. 5 ml of the digestion mixture (reagent 1) are added down walls of the flask and the whole content is allowed to stay for at least 1 h. 3. Then, the flask is heated in the digestion shelf to gradually increase the temperature to about 210°C, at the previously mentioned rate. 4. The flask along with its content is allowed to stay at the above temperature for about 10 h. After this period of time, the digestion is completed and from the acid mixture, only the sulfuric acid remains in the digest. 5. The flask is allowed to cool to room temperature. Then, 3 drops of water and concecutively 5 drops of concentrated hydrochloric acid are added directly to the bottom of the flask. 6. The flask is revolved by means of the hands, slowly along its elongated axis in such a way, so that the liquid digest to come into contact with the entire inner bulb area and lower neck of the flask. 7. The flask is loosely covered by its plastic stopper; it is heated to about 45°C by immersion in a thermostated bath and allowed to stay for about 30 min, in order to convert oxidized selenium entirely into selenites. 8. The flask is removed from the bath. Then, 5 ml of water and 2-3 drops of the indicator (reagent 2) are added to the digest. Swirling the content of the flask continuously, ammonium hydroxide solution (reagent 3) is added using a burette, till the indicator color change from pale red to light yellow (usually 6-7 ml). 9. To the resulted content of the flask, 5 ml or EDTA solution (reagent 4) and 1.5 ml of DAN solution (reagent 7) are added in sequence and then the flask is placed in the thermostated bath warmed up under the same conditions as those of the stage 7, to get the piazselenol. 10. The flask is cooled down using flowing tap water and then a calculated amount of water (usually 2-3 ml) is added to obtain a 20 ml solution. Then, 10 ml of cyclohexane (reagent 6) are added, the flask is waterproofed by its stopper and it is strongly shaked for at least 2 min according to the usual extraction technique. The flask is preferentially placed in darkness and it is allowed to stay for at least 15 min. 11. Most of the cyclohexane layer is taken off by a piston pipette; the lowest part of this layer is discharged to get rid of the possible water residues and the rest of the cyclohexane is transferred to a stoppered tube. This extract stays for about 2 h preferentially in darkness and then it is ready to be measured fluorometrically.

Results and discussion

The most critical points of the selenium analysis in general and more specifically in biological materials, are essentially the following: The possible selenium losses in all of the stages up to the end of the digestion and the factors affecting the determination up to the final stage of the measurement.

Thus, the method that has been formulated, took into account principally these two critical points and it was based on a series of evaluations, some of which were considered not to require verifications.

On the other hand, as it refers to the results shown in the tables, these are the mean values from five independent analyses of the same sample, expect if it is otherwise stated. It is also noted, that the deviations among the independent measurements never exceeded 2.5%.

1. Selenium losses during the digestion. In the wet digestion process of biological materials, charring appears ussually as an intermediate stage before the digestion to be completed, followed by vigorous oxidation caused by the acid mixture. But as both charring and vigorous oxidation, at least during the wet digestion with nitric-perchloric acids, can lead to significant selenium losses[8,14], it is pointed out that the precautions taken to avoid these losses during digestion, are not necessary as far as mainly no charring takes place.[8]

Thus it seemed, that the charring during such a digestion could be avoided by adjustment of the digestion conditions generally and especially the qualitative and the quantitative composition of the acid mixture, the order of the acid addition and mainly the rate of the temperature increase at least at the critical stages.

The above assessments led us to the proposed digestion procedure, the application of which was tested in a series of experiments using standard solutions only. As it was confirmed by the results, that are not presented, the digestion for a period of about 15 h, at a temperature of about 250°C does not lead essentially to selenium losses. On the contrary, the results were lower than expected, when the temperature was increased to about 290°C. However, the latter irregularity could most of the times be overcome, if after the stage 4 of the procedure, the neck of the flask was thoroughly rinsed by water in order any residue to be transferred to the flask bulb, while other times the above rinsing was impro-

ving only the recovery. This last finding was considered as strong evidence, that the volatile oxidized selenium forms at the relatively elevated temperature, find themselves on the upper parts of the inner walls of the flask neck, leading unavoidably to selenium loss.

Taking into account the above findings, the temperature during the digestion is not allowed to exceed 210°C, so that not only to exist a wide sefety margin to avoid selenium losses, but at the same time to ensure complete essentially removal of nitric and perchloric acids from the digest, leaving it in a medium of sulfuric acid.

On the other hand, experiments were carried out in biological samples, in order to search, if the proposed digestion procedure could cause charring. As it was found, there was no indication of charring, at least macroscopically, so that to consider favorable the entire of the suggested digestion conditions.

2. Cleaning of the glassware. As it was noticed during preliminary experiments, the more times the glassware was used, not only the higher but also the more abnormal the blank values were, although all of the glasswere before its use was carefully cleaned by the usual procedures.

Similar abnormalities were noticed by Grant[8] as a result of some unidentified substances present in the laboratory space.

As it was considered, the observed abnormalities were possibly due to glassware contamination by fluorescent substances remaining from previous analyses, not possible to remove completely even after careful cleaning, so that to be suggested the decomposition of these substances. To verify the above, indicative analyses were carried out after cleaning all of the glassware by persistent and prolonged heating all of the glassware into a strong acid medium. As it was confirmed, these abnormalities did not appear again.

3. Recovery in biological materials. Two series of various biological materials were analysed, adding in one only of these series, known amounts of selenium.

The relative results in table I show that the recoveries vary only between 98.9% and 100.7%;a strong evidence certainly that the results obtained by the proposed method could be considered accurate.

TABLE I. Recovery of Added Selenites in Various Biological Materials Applying the Proposed Analysis Scheme.

Sample	Selenium concentration found, ng/g		Recovery, %
	No addition	Addition of 100 ng	
Barley seeds, No 23	35.0	133.8	99.1
" " " 58	24.5	125.3	100.6
" " " 102	33.2	131.8	98.9
Alfalfa meal, " 152	77.8	179.1	100.7
" " " 187	103.7	203.1	99.7
" " " 201	83.6	182.7	99.5
Sheep wool, " 815	101.5	200.9	99.7
" " " 832	132.0	229.5	98.9
" " " 861	117.3	218.2	100.4

4. Reproducibility of the results. The reproducibility of the results taken by the proposed analytical scheme, was examined by performing 11 determinationsof the same sample either in a standard solution or in a biological material.

The selenium content found in a standard selenite solution of 250 ng and the resulted statistical data were as follows:

Found, ng 249.3, 252.0, 246.8, 254.0, 250.4, 247.6, 248.0, 250.8, 246.3, 252.4

Mean value, $\bar{x}$ =250.09, n=11, Relative Standard Deviation, RSD=1.074%

Standard Error of the Meam, SEM, $\sigma m=\sigma/\sqrt{n}=\pm 0.81021$

Relative Standard Error, RSE, $\sigma/\sqrt{n}/\bar{x}=0.00324$

On the other hand, the selenium content in an alfalfa leaves sample and the resulted statistical data, were as follows;

Found, ng 153.4, 151.6, 153.8, 151.0, 154.0, 153.0, 154.8, 150.4, 153.0, 151.0, 149.4

Mean value, $\bar{x}$=152.31 n=11 RSD=1.127%

SEM=±0.51759 RSE=0.00340

The above finfings show among the others that the RSD in both cases are less than 2%.

5. Selenium determinations in biological materials. The formulation of the proposed analytical scheme was applied in various biological materials,for indicative only purpose. The obtained results are shown in table II.

TABLE II. Selenium Determination in a Variety of Biological Materials According to the Proposed Analysis Scheme.

Sample	Selenium concentration ± $ts/\sqrt{n}$ *,**
Sheep whole blood, sample No 315	68.3 ± 1.2 *
" " " " " 338	51.0 ± 0.9 *
" " " " " 381	93.8 ± 1.6 *
Sheep liver, " " 507	336.5 ± 5.2 **
" " " " 521	234.1 ± 3.6 **
" " " " 555	282.7 ± 4.4 **
Soya meal, " " 302	317.2 ± 4.9 **
" " " " 310	286.6 ± 4.5 **
" " " " 332	330.6 ± 5.1 **
Corn seeds " " 167	21.2 ± 0.4 **
" " " " 174	14.5 ± 0.3 **
" " " " 181	17.8 ± 0.3 **

* ng/ml, ** ng/g dry matter. The results are the mean values of n=5 independent determinations with a confidence level of 95%.

CONCLUSIONS

The selenium determination, according to the proposed analytical scheme, has given notably accurate and reproducible results for a variety of biological materials. The digestion procedure as well as the order of the reagent addition, along with the precautions taken throughout the work, were responsible for the above results.

ACKNOWLEDGMENTS

We are grateful to the Clinical Pathology of Veterinary Department, Aristotelian University of Thessaloniki for the facilities offered to carry out the experiments.

SUMMARY

IMPROVED PROCEDURE FOR THE FLUOROMETRIC DETERMINATION OF SELENIUM IN BIOLOGICAL MATERIALS

A. AYIANNIDIS* and A. VOULGAROPOULOS**

* Chemistry Lab. of Veterinary Dept., Aristotelian University of Thessaloniki.

** Analytical Chemistry Lab. of Chemistry Dept., Aristotelian Univerity of Thessaloniki.

An analysis scheme for the determination of selenium in biological materials has been developed. The thermostated wet digestion of the sample, carried out in Kjeldhal flasks by a mixture of nitric - perchloric - sulfuric acids as well as the sample preparation are described. The Relative SD of the results taken according to the suggested method, is not more than 2% for amounts up to about 300ng. The method was tested indicatively in various biological materials.

ΠΕΡΙΛΗΨΗ

ΒΕΛΤΙΩΜΕΝΗ ΜΕΘΟΔΟΛΟΓΙΑ ΓΙΑ ΤΟΝ ΦΘΟΡΙΣΜΟΜΕΤΡΙΚΟ ΠΡΟΣΔΙΟΡΙΣΜΟ ΤΟΥ ΣΕΛΗΝΙΟΥ ΣΕ ΒΙΟΛΟΓΙΚΑ ΥΛΙΚΑ

Αναπτύχθηκε αναλυτικό σχήμα για τον προσδιορισμό του σεληνίου σε βιολογικά υλικά. Περιγράφονται η θερμοσταιούμενη διάταξη και η μεθοδολογία της υγρής πέψης με μίγμα οξέων νιτρικού υπερχλωρικού και θειικού σε φιάλες Kjeldahl καθώς και η προετοιμασία του δείγματος. Η Σχετική Τυπική Απόκλιση, RSD, των αποτελεσμάτων δεν υπερβαίνει το 2% για περιεκτικότητα των δειγμάτων σε σελήνιο μέχρι 300 ng περίπου. Η μέθοδος δοκιμάστηκε σε ποικιλία βιολογικών υλικών.

REFERENCES

1. Underwood, E.J., in *"Trace Elements in Human and Animal Nutrition"*, Academic Press Inc., London, 1971, p.323.
2. Rosenfeld, J., and Beath, O.A., in *"Selenium Geobotany, Biochemistry, Toxicity and Nutrition"*, Academic Press, New York, 1964.
3. Spais, A., Papasteriadis, A., Agiannidis, A., Roubies, N.,Giantzis,N. and Argyroudis, S., Proceedings of the International Congress *"Trace Elements Metabolism in Man and Animals"* (Tema-3), München, 1977, p. 501.
4. Spais, A., Papasteriadis, A., Giantzis, N., Paschaleries, G.,Agiannidis, A., Roubies, N., and Omirou, A., Summary proccedings of the 21st International Veterinary Congress, Moscow, 1979, vol.6 part XII,p.12.
5. Lott, P.F., Cukor, P., Moriber, G., and Sloga, J., Anal. Chem., 1963, 35, 1159.

Chimika Chronika, New Series, 19, 119-124(1990)

SYNTHÈSE DE QUELQUES DÉRIVÉS DE LA RIMANTADINE AVEC UNE ACTIVITÉ ANTIBACTÉRIENNE

SPYROULA GAROUFALIAS, EVANGELOS COSTAKIS

Laboratoire de Pharmacie chimique, 104 rue Solonos, GR-106 80, Athènes (GRÈCE)

H. TUMAH, N. LEGAKIS

Laboratoire de Microbiologie, Université d'Athènes Goudi-Athènes 115 27 (GRÈCE)

Dérivés de la rimantadine

RÉSUMÉ

Dans le présent travail nous decrivons la synthèse de la N-[(dimethylaminoethoxy) acétyl]-a-méthyl-adamantane-1-méthylamine *1* et de la N-(dimethylaminoacétyl)-a-méthyladamantane-1-méthylamine *2*. Les dérivés ci-dessus ont été transformés en sels de bromure d'ammonium quaaternaire qui ont été testés pour leur activité antibactérienne.

KEYWORDS

Quaternary ammonium salts of rimantadine derivatives. Antibacterial activity.

INTRODUCTION

Il est connu que plusieurs dérivés adamantaniques présentent une activité antivirale et antimicrobienne[1-6]. Parmi ceux ci la a-méthyladamantane-1-méthylamine *I* (rimantadine)[1] et la [(diméthylamino)-2-éthoxy]-1, acétamide *II* (tromantadine)[2,3] possèdent une activité antivirale considérable et présentent une analogie structurale avec les dérivés *1* et *2* que nous avons synthétisés. (Schema 1)

Afin d'obtenir une meilleure activité antibactérienne nous avons transformé les dérivés *1* et *2* en sels d'ammonium quaternaire[7,8] en les faisant réagir avec des bromures d'alkyles d'un poids moléculaire relativement élevé.

PARTIE-CHIMIQUE

La synthèse de la N-[(dimethylaminoéthoxy)-acétyl]-α-méthyl-adamantane-1-méthylamine *1* et de la N-(dimethylaminoacétyl)-α-méthyl-adamantane-1-methylamine *2.* figure dans le schéma I. Comme produit de départ nous avons employé l'oxime d'adamantyl-1-méthylcétone 4[1,9] dont la réduction fournit la a-méthyl-adamantane-1-méthylamine *5*[1] qui avec l'action du chlorure de chloracétyle se transforme en N-(chloracetyl)-a-méthyladamantane-1-méthanamine *6*. Ce chloracétamide *6* réagit d'une part avec le diméthylaminoethanol sodé et fournit l'éther *1*, et d'autre part avec la diméthylamine et fournit l'amide *2.* Le traitement des composés *1* et *2* avec des bromures d'alkyles d'un poids moléculaire élevé conduit aux sels d'ammonium quaternaire correspontants. La structure des produits *6 1* et *2* a été confirmée par des analyses élémentaires satisfaisantes ainsi que par la spectroscopie I.R et RMN. Les constantes physiques des sels d'ammonium quaternaires sont donnés, dans les tableaux I et II.

PARTIE-EXPÉRIMENTALE

Les points de fusion des produits préparés dans le présent travail ont été déterminés dans les tubes capillaires de l'appareil de Büchi et ils ne sont pas corrigés. Les analyses élémentaires ont été réalisées par le Centre de Microanalyse du C.N.R.S (France) et sont conformes aux valeurs théorique á ±0,4%. Les spectres IR ont été obtenus avec le specktrophotomètre Perkin-Elmer 177 et les spectres RMN avec le spectrophotemètre Varian FT-80A dans $CDCl_3$ en utilisant le TMS comme référence interne. L'adamantyl-1-méthylcétone *3* a été préparée en utilisant la méthode des H. Stetter et E. Rauscher[7] L'adamantyl-1-méthylcétoxime *4* a été synthétisée selon les procédés classiques[1]. La syntèse de la α-méthyladamantane-1-méthylamine *5* (rimantadine) a été effectuée par réduction de l'oxime précedente avec le $LiAlH_4$[1].

N-(chloracétyl)-α-méthyladamantane-1-méthanamine 6

Dans une solution de 5,53 g (0,0308 mole) de a-méthyladamantane-1 méthylamine *5* dans 50 ml de chloroforme on ajoute une suspension de 3,6 g (0,034 mole) de carbonate de sodium dans 5 ml d'eau, puis à goutte à goutte et sous agitation vigoureuse 3,84 g (0,034 mole) de chlorure de chloracétyle. Après addition, on poursuit l'agitation pendant *1/2* h, on sépare la couche chloroformique et on extrait une fois la couche aqueuse au chloroforme. Les couches chloroformiques unies sont lavées á l'eau, séchées sur Na_2SO_4 et évaporées.

On obtient un produit huileux qui se cristallise après refroidissement Rdt: 6,5 g (82%).

F = 110-112°C.
IR(Nujol), v(NH) 3280 cm^{-1}, v(C=0) 1650 cm^{-1}. RMN ($CDCl_3$) δ(ppm): 1,10 (d, 3H, J = 6Hz, $C\underline{H}_3CH$), 1,25-2,32(m, 16H $CH_3C\underline{H}$, adamantaniques-H), 4,08 (s, 2H, $C\underline{H}_2Cl$).

N-[(diméthylaminoéthoxy) acétyl]-a-méthyl-adamantane-1-méthylamine-1

On chauffe jusqu à dissolution compléte du sodium 1,53 g (0,017 mole) de diméthylaminoéthanol et 0,3 g (0,017 gratom) de sodium dans 80 ml de xylène anhydre. Après refroidissement on y ajoute goutte à goutte et sous agitation 4 g (0,015 mole) de N-(chloracétyl)-α- méthyladamantane-1- méthanamine *6* en solution dans 80 ml de xylène anhydre. Le mélange est porté a l'ébullition pendant 20h, après quoi on y ajoute de l'eau, il sépare la couche organique et extrait la couche aqueuse à l'éther.

Les couches organiques unies sont lavées à l'eau puis extraites au HCl á 5%. La couche aqueuse est alcalinisée avec du carbonate de sodium et extraite deux fois á l'éther. Les couches éthérées unies sont lavées á l'eau, séchées sur Na_2SO_4 et evaporées. On obtient 2 g de produit huileux soit un rendement de 41% IR (Nujol), v(NH) 3310 cm^{-1}, v(C=0) 1660 cm^{-1}. RMN ($CDCl_3$) δ(ppm) 1,05(d, 3H, J=6Hz, $C\underline{H}_3$ CH), 1,30-2,50 (complex m, 18H, $CH_3C\underline{H}$, $C\underline{H}_2N$, adamantaniques-H), 2,15 (s, 6H, $(CH_3)_2N$), 3,10 (t, 2H, J=7Hz, OCH_2CH_2N), 3,65 (s, 2H, $COC\underline{H}_2O$).

Méthode generale de préparation des sels de bromure d'ammonium quaternaire 1'

On porte pendant 10h á l'ébullition une solution acétonique de 0,009 mole de base *1* et de 0,018 mole de bromure d'alkyle. Après évaporation de l'acétone on recristallise dans un mélange acétone anhydre-éther anhydre.

Rendement 80%

Les constantes physiques des sels préparés sont données dans le tableau I.

Tableau I

N-(diméthylaminoacétyl)-α-méthyl-adamantane-1-méthylamine-2

On agite un mélange de 10 ml d'une solution éthanolique de diméthylamine et d'une solution de 3 g (0,012 mole) du chloracétamide *6* dans 30 ml d'éthanol pendant 5 jours. Le mélange est par la suite chauffé légèrement pendant 1 heure et évaporé jusqu' à sec sous pression reduite. On ajoute de l'eau et on extrait a l'éther. La couche éthérée est par la suite extraite á l'acide chlorhydrique á 5%. On alcalinise les couches aqueuses avec du Na_2CO_3 et on extrait à l'éther. On lave a l'eau les couches éthérées unies, les séche sur Na_2SO_4 et les évapore. Le residu cristallise par refroidissement. Rdt: 3 g (96%)
F = 55-58°C (n-héxane). IR (Nujol), v(NH) 3310 cm^{-1},
V(C=0) 1670 cm^{-1} RMN($CDCl_3$) δppm 1,05 (d, 3H, J=6Hz, $C\underline{H}_3CH$), 1,30-2,25 (m, 16H, CH_3 $C\underline{H}$, adamantaniques -H), 2,30(s, 6H, $(C\underline{H}_3)_2N$) 2,94 (s, 2H, $C\underline{H}_2$ CO) 3,45-4,00 (br s, 1H, NH). La base *2* est transformée en sels

d'ammonium quaternaire en utilisant la méme méthode que pour la base *1*. Les analyses et les constantes physiques de ces sels sont données dans le tableau *II*.

Tableau II

Etude del'activité antibactérienne

Nous avons controlé les substances synthétisées par leur activité antibactérienne in vitro sur quatres espèces différentes: Staphylococcus aureus (ATCC No 9144), Streptococcus faecalis (ATCC No 10541) et Escherichia coli (CCM No 5172), Pseudomonas aeruginosa (CCM No 1960).

Nous avons utilisé la méthode de concentration minimum inhibitrice (mg/ml) (CMI) (la plus petite concentration de substance donnant une inhibition de la croissance)$_{(10)}$. La concentration finale des bactéries était de l'ordre de 10^5, l'observation, des résultats étant éffectuée aprés 18-24 h d'incubation á la température de 37^0C. Les résultats sont résumés dans le tableau III.

Tableau III

Particulièrement pour les sels d'ammonium quaternaire des substances 1 et 2 nous observons une augmentation de l'activité proportionelle au nombre des atomes du carbone du groupement alkyle. L'activité était plus importante pour les cocci Gram possibifs (st. aurens et str. faecalis).

SUMMARY

Rimantadine derivatives

In this paper the synthesis of rimantadine derivatives is described. Actually the quaternary ammonium bromides of N-[(dimethylaminoethoxy) acetyl]-α-methyl-1-adamantanemethylamine *1* and N-(dimethylaminoacetyl)-α-methyl-1- adamantanemethylamine *2* have been synthesized. The above mentioned products exhibit an antibactérial activity, especially agains Gram-possitive grains, which increases acording to the number of the alkyl group's carbon atoms of the quaternary ammonium.

ΠΕΡΙΛΗΨΗ

Παράγωγα της ριμανταδίνης

Στην παρούσα εργασία περιγράφεται η σύνθεση παραγώγων της ριμανταδίνης. Συγκεριμένα παρασκευάστηκαν τα βρωμιούχα άλατα του τεταρτοταγούς αμμωνίου της N-[(διμεθυλαμινοαιθοξυ)ακετυλο]-α-μεθυλο-1-αδαμαντομενθυλαμίνης *1* και της N-(διμεθυλαμινοακετυλο)-α-μεθύλο-1-αδαμαντονομεθυλαμίνης *2*. Τα ανωτέρω προϊόντα εμφανίζουν αντιβακτηριακή δράση και ιδιαίτερα έναντι των Gram θετικών κόκκων, η οποία

αυξάνεται με τον αριθμό των ατόμων άνθρακα του αλκυλίου της ομάδας του τεταρτοταγούς αμμωνίου.

BIBLIOGRAPHIE

1. Aldrich P. Hermann E. Meier W. Paulshock M. Prichard W. Snyder J. et Watts: J. *Med. Chem 14* 535 (1971).
2. Scherm A. et Peteri D. Ger offen 2, 316, 839: Chem Abstr., *82* 16618 m (1975).
3. Scherm A. et Peteri D. Ger Offen 1,941,218: Chem. Abstr., *74* 99516 K (1971).
4. Antoniadou-Vysas A. Foscolos G. et chytirogou-Ladas A.: *Eur. J. Med. Chem 21* 73 (1966).
5. Garoufalias S. Vyzas A. Fytas G. Foscolos G.B. et Chytiroglou-Ladas A: *An. Pharm. Fr. 46* 97(1988).
6. Drugs of the future Vol. *8* No 3, p. 167 (1984).
7. Hamilton W.A (1971) Membrane active antibacterial compounds. In inhibition and Destruction of the Microbial Cell p. 77-93 London: Academic Press.
8. Hugo W.B. (1965) Some aspects of he action of Cationic Surface-active agents on microbial cells with special reference to they- action on enzymes. Surface Activity and the Microbial cell. SCI Monograph 19, p 67-82 London: Society of Chemical Industry.
9. Stetter H. et Rausher E.: *Ber 93* II 2054 (1960).
10. National Committee for clinical Laboratory Standards (1983) Standard methods for dilution antimicrobial susceptibility tests for bacteria that grow aerobically. M7-T. National Commitée for clinical Laboratory Standards, Villanova, Pa.

TABLEAU I: Sels d'ammonium quaternaire de N-[(diméthylaminoéthoxy)-acétyl]-α-méthyl-adamantane-1-méthylamine *1*.

Formule 1

n	F°C*	Formule brute	Analyses C Calc%	C Tr%	H Calc%	H Tr%
3	157-180	$C_{22}H_{41}N_2O_2Br$	59,31	59,23	9,28	9,25
6	167-169	$C_{25}H_{47}N_2O_2Br$	61,58	61,43	9,72	9,66
7	168-170	$C_{26}H_{49}N_2O_2Br$	62,25	61,80	9,85	9,68
8	141-143	$C_{27}H_{51}N_2O_2Br$	62,89	62,89	9,97	10,12
9	128-130	$C_{28}H_{53}N_2O_2Br$	63,50	63,82	10,09	10,09

* Recrystallisation dans l'acétone-éther.

TABLEAU II: Sels d'ammonium quaternaire de N-(diméthylaminoacétyl)-α-méthyl-adamantane-1-méthylamine *2*.

Formule 2

n	F°C*	Formule brute	Analyses C Calc%	C Tr%	H Calc%	H Tr%
7	119-121	$C_{24}H_{45}N_2OBr$	63,00	62,60	9,91	9,87
9	122-124	$C_{26}H_{49}N_2OBr$	64,30	63,90	10,17	10,06
11	114-116	$C_{28}H_{53}N_2OBr$	65,47	65,25	10,40	10,45

* Recrystallisation dans l'acétone-éther.

TABLEAU III: Activité antibactérienne

Produit testé	Concentation minimum inhibitrice CMI (mg/ml) Staphylococcus aureus	Streptococcus faecalis	Escherichia coli	Pseudom. aerugin.
1(n=3)	200	200	>200	>200
1(n=6)	25	100	>200	>200
1(n=7)	6,25	100	>200	>200
1(n=8)	6,25	25	50	100
1(n=9)	1,5	6,25	50	50
2(n=7)	12,5	12,5	50	>50
2(n=9)	3,1	6,25	50	50

GUIDE TO AUTHORS

Since January 1,1988, all contributions to Chimika Chronika, New Series are reproduced from camera-ready typescripts prepared by the authors.

Scope and Editorial Policies. — This International edition invites original contributions on research in all branches of chemistry and related sciences at the molecular level. Negative results will only be accepted when they can be considered to contribute significantly by the science. In the selection by the editors of manuscripts for publication, emphasis is placed on the quality and originality of the work.

Papers should be written in English. Authors need not be members of the Greek Chemists Association.

Manuscripts are classified as (normal length) *papers, short papers or notes, preliminary communications or letters, and reviews. A short paper* is a concise but complete description of a small, rounded off investigation or of a side part from the main line of investigation, which will not be included in a later paper. It is not a portion of work, that can be more suitably incorporated in a normal length paper, after the investigation has progressed further.

As *Notes* are characterized short papers on limited facets of an investigation e.g. describing a useful modification of an experimental technique or method, reporting additional data and eventually, more precise values for measurements already existing in the literature, and so on.

A *Preliminary Communication* is a brief report of work, which will be included in a later normal length paper. Criteria for its publication are first, when it is considered that the science would be advanced if results were made available as soon as possible to others working on the same subject and second, for the protection of priority for the author. Every effort is made in order to publish preliminary communications as soon as possible and it would help the editors if the author, in a covering letter, were to give his reasons for believing that publication is urgent. Although extensive references to the earlier literature are not usually needed, the most recent papers on the same subject should be referred to, and sufficient experimental details should be given so that those familiar with the subject can immediately repeat the experiments. In general, preliminary communications should be more than an abstract or a summary.

As *Letters* are characterized any other types of communications, previously included in the terms "letter to editor" or "communication to editor", but not fulfilling the criteria mentioned above for a preliminary communication or a note, or dealing with scientific criticism of published work in this (or other) journals.

Reviews should be fully comprehensive on a narrow field of specialized research, expected to be interesting for a broad number of scientists: they are invited papers, otherwise submitted after contracting the editors.

Organization of Manuscripts. — Athors should submit *three copies* of the manuscript in double-spaced typing on the one side of pages of uniform size, with a margin 5 cm wide on the left; this applies also to summaries (english and greek), references and notes.

Every manuscript should begin with a *Cover Page* and attached to it on a separate sheet, the *Acknowledgments* and notice of grant support (if appropriate).

The cover page should contain the title, the name(s) of author(s) (first-name in full, middle, surname), the name and address of laboratory of research, the footnotes to the title and/or to an author's name (both made with asterisks), and the name and address of the recipient correspondence. It should also contain a Running Title, not exceeding 40 letters.

The purpose of this arrangement is to facilitate the reviewing procedure, which is based on a protective anonymity between reviewers and authors, closen in order to meet the requirements of a highly objective selection of papers to be published in this journal, and to increase the validity of criticisms. Cover page and aknowledgements are not sent to reviewers and accordingly, sentences in firs person accompanied by literature references to earlier papers of the author(s) should be completely avoided in the text.

The next pages of the manuscript should be numbered in one consecutive series by the following sequence:

Page 1. — *Title* followed by a *summary* in English. The title should consist of carefully selected and properly presented key words which clearly identify the subjects considered in the paper. The *summary* should be as brief as possible but intelligible in itself, without reference to the paper, and containing sufficient information to serve as an *abstract.*

Every *summary* should end with up to ten *key words,* necessary to direct the attention of abstracting services and readers to subjects in the article that are not referred to in the title.

Page 2. — *Abbreviations* and *Terminology,* i.e. a list of all abbreviations and unusual terms used in the paper; it may include the systematic name of any compound, mentioned in the text by a shorter "trivial" or "common" name.

Page 3 and subsequent. — The text divided into sections and, if necessary, subsections. The first section of a normal-length paper is always an *Introduction* stating the reasons for performing the work, with brief reference to previous work on the subject; the background discussion should be restricted to pertinent material, avoiding an extensive review of prior work; and documentation of the literature should be selective rather than exhaustive, particularly if reviews can be cited.

The arrangement of the text after the introduction is left to the author(s). The order *Materials, Methods, Results and Discussion,* with headings, subheadings and sideheadings chosen by the author(s), is usually the most satisfactory. However, in lengthy papers (usually, of synthetic work) the manuscript may be organized so that the principal findings and conclusions are concisely presented in an initial section (Theoretical Part), with supporting data, experimental details, and supplementary discussion in a separate section (Experimental Part).

Photocopies of tables, figures, legends, footnotes etc should be pasted on the appropriate place, so that each page will be ready for reproduction. The size of letters chosen for the original should be legible after 20% reduction during reproduction.

Subsequent Pages — After the text pages separate sheets should be used for the following: a) greek summary; b) references and notes.

The *greek summary,* headed by a greek translation of the title, should be extensive and may refer to literature citations and to tables or figures of the paper, in order to give a brief but factual account of the contents and conclusions of the paper, and of its relevance; for this purpose, it may exceed half printed page. In its place, foreign authors may submit an extensive summary in english, which will be gladly translated into greek by care of the editors.

References and Notes, as already mentioned, should be brought together at the end of the paper in one consecutive series by order of citation in the text (not in alphabetical order). Authors should check whether every reference in the text appears in the list and *vice versa.* References to papers "in press" imply that the paper has been accepted for publication and, therefore, the name of the journal should be given. References to a "personal communication" (never "private") will be accepted only when the author submits written permission of the worker concerned. References should be listed according to the following style:

For journal articles: Last name(s) of author(s) and initials: *Name of journal* (abbreviated according to Chemical Abstracts, Service Source Index (CASSIS) 1907-1984, *Volume number,* First page of article, Year in parentheses.

Example: 1 Smith, J.B. and Jones, A.B.: *J. Am. Chem. Soc.* **47,** 115 (1945).

For books and monographs: Author's names as above: *Title of book,* (Number of edition), Page, Publisher, City, Year of edition.

Example: 2 Smith, J.B.: *Organic Chemistyr,* (2d edition), p. 57, Wiley, London (1945).

For multi-author volumes (Articles in books): Authors' names as above: Name of editor(s): *Name of book* Volume number Part number, Page(s), Publisher, City, Year of edition.

Example: 3 Smith, J.B.: Jones, A.B.: *Organic Chemistry,* Vol. 5. Part A, p. 57 (or pp. 46-62), Elsevier, Amsterdam, 1953.

Manuscripts for short papers and preliminary communications should be organized on the same principles. Besides some minor modifications in their published form, they differ from a normal length paper in that the headings and subheadings in the text, as well as the summary preceeding the text are ommitted. In these cases, the first paragraph of the text may serve the purpose of an abstract, summing up very briefly the scope and the main findings and conclusions of the investigation. However, for reasons already mentioned, the text is always followed by a greek extensive summary.

After the paper is accepted for publication it is returned to the authors for the preparation of the final camera ready typescript. The authors are required to prepare the typescript on a special paper supplied by the Editing Commitee according to enclosed instructions.

Page Charge and Reprints. A page charge of 2000 drachmas or 20 U.S. dollars assessed to cover in part the cost of publication, plus the cost of 50 reprints, which will be mailed to the recipient correspondence without any additional requirement. However, papers are accepted or rejected only on the basis of merit and the decision to publish a paper is made before the charge is assessed.

CHIMIKA CHRONIKA, *NEW SERIES*

CONTENTS